

TECHNICAL
LIBRARY



TECHNICAL REPORT RL-80-9

LASER SPECKLE INTERFEROMETRIC THERMOELASTICITY

John A. Schaeffel, Jr.
Ground Equipment & Missile Structures Directorate
US Army Missile Laboratory

30 May 1980



U.S. ARMY MISSILE COMMAND

Redstone Arsenal, Alabama 35809

Approved for public release; distribution unlimited.

DTIC QUALITY INSPECTED 3

DISPOSITION INSTRUCTIONS

DESTROY THIS REPORT WHEN IT IS NO LONGER NEEDED. DO NOT RETURN IT TO THE ORIGINATOR.

DISCLAIMER

THE FINDINGS IN THIS REPORT ARE NOT TO BE CONSTRUED AS AN OFFICIAL DEPARTMENT OF THE ARMY POSITION UNLESS SO DESIGNATED BY OTHER AUTHORIZED DOCUMENTS.

TRADE NAMES

USE OF TRADE NAMES OR MANUFACTURERS IN THIS REPORT DOES NOT CONSTITUTE AN OFFICIAL INDORSEMENT OR APPROVAL OF THE USE OF SUCH COMMERCIAL HARDWARE OR SOFTWARE.

UNCLASSIFIED

SECURITY CLASSIFICATION OF THIS PAGE (When Data Entered)

REPORT DOCUMENTATION PAGE		READ INSTRUCTIONS BEFORE COMPLETING FORM
1. REPORT NUMBER TR RL-80-9	2. GOVT ACCESSION NO.	3. RECIPIENT'S CATALOG NUMBER
4. TITLE (and Subtitle) Laser Speckle Interferometric Thermoelasticity		5. TYPE OF REPORT & PERIOD COVERED Technical Report
		6. PERFORMING ORG. REPORT NUMBER
7. AUTHOR(s) John A. Schaeffel, Jr.		8. CONTRACT OR GRANT NUMBER(s)
9. PERFORMING ORGANIZATION NAME AND ADDRESS Commander, US Army Missile Command ATTN: DRSMI-RL Redstone Arsenal, AL 35809		10. PROGRAM ELEMENT, PROJECT, TASK AREA & WORK UNIT NUMBERS
11. CONTROLLING OFFICE NAME AND ADDRESS Commander, US Army Missile Command ATTN: DRSMI-RPT Redstone Arsenal, AL 35809		12. REPORT DATE 30 May 1980
		13. NUMBER OF PAGES 104
14. MONITORING AGENCY NAME & ADDRESS (if different from Controlling Office)		15. SECURITY CLASS. (of this report) UNCLASSIFIED
		15a. DECLASSIFICATION/DOWNGRADING SCHEDULE
16. DISTRIBUTION STATEMENT (of this Report) Approved for public release; distribution unlimited.		
17. DISTRIBUTION STATEMENT (of the abstract entered in Block 20, if different from Report)		
18. SUPPLEMENTARY NOTES		
19. KEY WORDS (Continue on reverse side if necessary and identify by block number) Laser Speckle Thermostrain Thermal Deformation Interferometry Thermostress Experimental Mechanics Speckle Interferometry Thermoelasticity Experimental Stress Analysis Stress Analysis Isotherms <i>Laser Interferometry</i>		
20. ABSTRACT (Continue on reverse side if necessary and identify by block number) This report presents the theory for using laser speckle interferometry for making measurements in thermoelasticity problems. General thermoelastic theory, laser speckle interferometric theory, thermal stress deformation of thin plates, and numerical approximations to the thermostress equations are all projected. Two experimental examples are presented which involve the heating of a circular flat plate and the uniform heating of a metallic bar. Interferometrically obtained temperature measurements are compared with thermocouple data.		

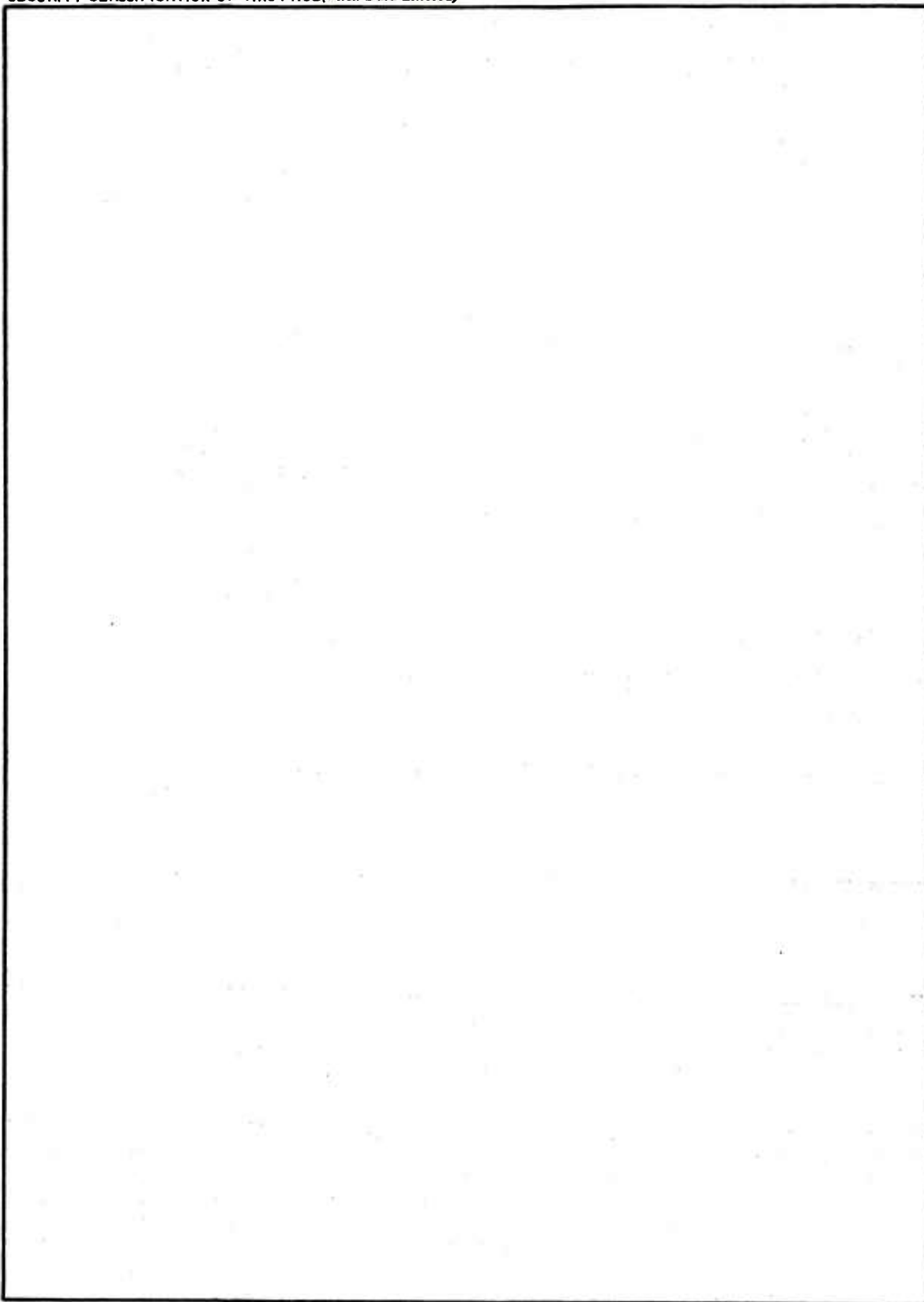
DD FORM 1 JAN 73 1473

EDITION OF 1 NOV 65 IS OBSOLETE

UNCLASSIFIED

SECURITY CLASSIFICATION OF THIS PAGE (When Data Entered)

SECURITY CLASSIFICATION OF THIS PAGE(When Data Entered)



SECURITY CLASSIFICATION OF THIS PAGE(When Data Entered)

ACKNOWLEDGMENT

The author sincerely wishes to express his gratitude to Mrs. Alison S. Dempsey and Mr. Robert B. McGowan for their assistance in this project.

CONTENTS

	<u>Page</u>
I. INTRODUCTION	5
II. THEORETICAL ANALYSIS	5
A. GENERAL THERMOELASTICITY THEORY	5
B. LASER SPECKLE INTERFEROMETRY THEORY	17
C. THERMAL EXPANSION OF A HEATED ROD	21
D. THERMAL STRESS DEFORMATION OF A THIN CIRCULAR PLATE NEGLECTING THE z COMPONENT OF DEFORMATION	23
E. THERMAL STRESS DEFORMATION OF A THIN CIRCULAR PLATE WITH A CORRECTION FOR THE z COMPONENT OF DEFORMATION	26
F. THIN PLATE THERMOSTRESS EQUATIONS IN RECTANGULAR COORDINATES	31
G. NUMERICAL DIFFERENTIATION OF THE THERMAL INDUCED DEFORMATION FIELD TO PREDICT TEMPERATURE CHANGE	33
H. DEFORMATION OF CIRCULAR FLAT PLATES IN CYLINDRICAL COORDINATES	34
I. GENERAL THERMOSTRESS EQUATIONS FOR THIN PLATES IN RECTANGULAR COORDINATES	42
J. THERMAL STRESS DEFORMATION OF A THIN CIRCULAR PLATE WITH A MODIFIED CORRECTION FOR THE z COMPONENT OF DEFORMATION	44
K. LEAST SQUARES METHOD OF DIFFERENTIATING EXPERIMENTAL DATA	49
L. POLYNOMIAL APPROXIMATION TO THE THIN PLATE THERMOSTRESS EQUATION IN CYLINDRICAL COORDINATES	52
III. EXPERIMENTAL EXAMPLES	54
A. COMPUTER SYSTEM FOR ANALYZING LASER SPECKLE INTERFEROGRAMS	54
B. TEMPERATURE CHANGE MEASUREMENTS FOR A HEATED CIRCULAR FLAT PLATE (CASE I)	54
C. TEMPERATURE CHANGE MEASUREMENTS FOR A HEATED COPPER BUS BAR (CASE II)	78
D. TEMPERATURE CHANGE MEASUREMENTS FOR A HEATED CIRCULAR FLAT PLATE (CASE III)	83
IV. CONCLUSIONS	86
REFERENCES	87
APPENDIX	89

ILLUSTRATIONS

	<u>Page</u>
1. Differential Stress Element With Unit Normals n_x, n_y, n_z . . .	10
2. Laser Speckle Interferometry Configuration	18
3. Diffraction Halo Geometry	19
4. Thermal Expansion of a Uniformly Heated Rod	21
5. ΔT Versus $\Delta \epsilon$ for Various Rod Lengths (L), $\alpha = 1.66 \times 10^{-5} \text{ } ^\circ\text{C}^{-1}$	22
6. Thermal Stress Deformation of a Thin Circular Plate With ρ_r and ρ_z Components of Deformation	27
7. Assumed Deformation Profile in the z Direction of a Heated Flat Plate	29
8. Geometry for Measuring Temperature Change ΔT at Location i,j	33
9. Coordinates for a Circular Plate	45
10. System Used to Analyze Laser Speckle Interferograms	55
11. Basic Laboratory Configuration for Examining the Deformation of Circular Heated Flat Plates	56
12. Circular Flat Plate	57
13. Heater Element Support	58
14. Plate Heater Unit Holder	60
15. Heater Unit Support Base	61
16. Attachment of Iron-Constantan Thermocouples to Aluminum Plate	62
17. Complete Assembly of Thermocouples on the Circular Flat Plate	63
18. Thermocouple Switch Network Schematic	64
19. Thermocouple Rotary Switch	65
20. Reference Junction Ice Bath	67
21. Leeds and Northrup 8690 Millivolt Potentiometer	68
22. Jodon ES-100 Electronic Shutter System	69
23. Case I $\gamma(r)$ Versus r	72
24. Illumination Direction for the Flat Circular Plate	74
25. Side View of Case I Experiment Illustrating the Laser, Heating System and Thermocouple Read-Out System	75
26. Case I Optical Configuration Without Cylindrical Lens Assembly	76
27. Back Side of Circular Flat Plate Illustrating Thermocouples	77
28. Copper Bus Bar in Glass Beaker Imersion Tank	79
29. Case II Laboratory Setup	80
30. Side View of Case II Experiment	81

TABLES

	<u>Page</u>
1. Case I Interferometric Data	71
2. Corrected Case I Interferometric Data	71
3. Case II Laboratory Data	82
4. Case II Temperature Measurement Results	83
5. Case I Test Data	83
6. Corrected Table 5 Data	84

I. INTRODUCTION

The thermoelasticity problems found in mechanics usually revolve around one of four areas:

1. The measurement of a body's surface temperature from its surface deformation field.
2. The measurement of thermal gradients at the surface of a body from its surface deformation field.
3. The measurement of thermal-induced deformation at the surface of a body.
4. The measurement of thermal-induced stress/strain at the surface of a body.

The objective of this report is to present the theory and experimental laser speckle interferometry techniques that were used to obtain these measurements. Section II lays the foundation for using the laser to make these noncontact measurements. Since laser speckle interferometry is used to measure in-plane motion only, certain restrictions have to be imposed on the theory.

Although the theory is developed for three dimensions, necessary simplifications are used to reduce this theory by one dimension. Section III consists of two sample problems that were used to test the theory of Section II. The thin circular flat plate and uniformly heated rod are treated in Section II. Section IV presents the conclusions drawn from this work.

II. THEORETICAL ANALYSIS

A. General Thermoelasticity Theory

The linear theory of elasticity may be used to predict the deformation field of a body resulting from thermal-induced stress and strain. A temperature change at an arbitrary location in a body may be predicted from the local deformation field. The theory to follow assumes that the body consists of an isotropic hookean material which obeys linear thermoelastic behavior. For anisotropic materials, the theory becomes significantly more involved and will not be treated in

this analysis. Much of the analysis will be presented in tensor form to simplify the work.

The strain displacement relations from the theory of elasticity may be expressed as

$$\epsilon_{ij} = \left\{ \frac{\partial U_i}{\partial x_j} + \frac{\partial U_j}{\partial x_i} \right\} - \delta_{ij} \frac{\partial U_i}{\partial x_j} \quad (1)$$

Equation (1) expresses the strain field ϵ_{ij} to the displacement field U_i in the rectangular coordinate system x_j . The equilibrium equations, which relate the stress field σ_{ij} and internal body forces B_i , may be expressed as

$$\frac{\partial \sigma_{ij}}{\partial x_j} + B_i = 0 \quad (2)$$

The following analysis was obtained from reference [1]. The boundary condition equation, which relates the stress $\vec{\sigma}_n$ on an arbitrary plane in a body to the body's internal stress field, is given as

$$\vec{\sigma}_n = \vec{\sigma}_i n_i \quad (3)$$

where n_i are the direction cosines of the plane. In expanded form, the components of Eq. (3) become

$$\sigma_{nx} = l\sigma_{xx} + m\sigma_{xy} + n\sigma_{xz}$$

$$\sigma_{ny} = l\sigma_{xy} + m\sigma_{yy} + n\sigma_{yz}$$

$$\sigma_{nz} = l\sigma_{xz} + m\sigma_{yz} + n\sigma_{zz} \quad .$$

For a body free of thermal-induced strain, the stress/strain relations may be expressed as

$$\epsilon_{xx} = \frac{1}{E} [\sigma_{xx} - \mu(\sigma_{yy} + \sigma_{zz})]$$

$$\epsilon_{yy} = \frac{1}{E} [\sigma_{yy} - \mu(\sigma_{xx} + \sigma_{zz})]$$

$$\epsilon_{zz} = \frac{1}{E} [\sigma_{zz} - \mu(\sigma_{xx} + \sigma_{yy})]$$

$$\epsilon_{xy} = \frac{1}{G} \sigma_{xy}$$

$$\epsilon_{yz} = \frac{1}{G} \sigma_{yz}$$

$$\epsilon_{zx} = \frac{1}{G} \sigma_{zx} \quad . \quad (4)$$

In Eq. (4), E is the modulus of elasticity, μ is poissons ratio, and G is a Lamé constant.

Using the general stress/strain relations and the concept of thermal-induced strains, the change in temperature ΔT in some local region Ω of a body may be related to the displacement field in the region Ω [1]. First, the thermal-induced strains for a body uniformly heated and subject to a free expansion is

$$\epsilon_t = \alpha \Delta T, \quad (5)$$

where ϵ_t is the local normal strain in any direction t of Ω , α is the coefficient of thermal expansion, and ΔT is the temperature change over Ω . The temperature coupled stress/strain relations are [1]

$$\begin{aligned} \epsilon_x - \alpha \Delta T &= \frac{1}{E} [\sigma_x - \mu(\sigma_y + \sigma_z)] \\ \epsilon_y - \alpha \Delta T &= \frac{1}{E} [\sigma_y - \mu(\sigma_z + \sigma_x)] \\ \epsilon_z - \alpha \Delta T &= \frac{1}{E} [\sigma_z - \mu(\sigma_x + \sigma_y)] \\ \epsilon_{xy} &= \frac{2(1 + \mu)}{E} \sigma_{xy} \\ \epsilon_{yz} &= \frac{2(1 + \mu)}{E} \sigma_{yz} \\ \epsilon_{zx} &= \frac{2(1 + \mu)}{E} \sigma_{zx} \end{aligned} \quad (6)$$

If all the stresses are temperature induced for a differential element with only thermal-induced strain, then

$$E\alpha\Delta T = \sigma_x - \mu(\sigma_y + \sigma_z) \quad (7a)$$

$$E\alpha\Delta T = \sigma_y - \mu(\sigma_x + \sigma_z) \quad (7b)$$

$$E\alpha\Delta T = \sigma_z - \mu(\sigma_x + \sigma_y) \quad ; \quad (7c)$$

then

$$3E\alpha\Delta T = (\sigma_x + \sigma_y + \sigma_z)(1 - 2\mu) \quad (8)$$

Subtract Eq. (7b) from Eq. (7a) and Eq. (7c) from Eq. (7b) to obtain

$$\sigma_x - \mu\sigma_y - \sigma_y + \mu\sigma_x = 0 \Rightarrow \sigma_x = \sigma_y$$

$$\sigma_y - \mu\sigma_z - \sigma_z + \mu\sigma_y = 0 \Rightarrow \sigma_y = \sigma_z$$

$$\therefore \sigma_x = \sigma_y = \sigma_z ,$$

or

$$\sigma_x = \sigma_y = \sigma_z = \frac{E\alpha\Delta T}{1 - 2\mu} . \quad (9)$$

Therefore, expansion of the differential element may be prevented by the application of a hydrostatic stress:

$$\sigma_t = \frac{-E\alpha\Delta T}{1 - 2\mu} . \quad (10)$$

The equilibrium equations, Eq. (2), without body forces present take the form

$$\begin{aligned} \frac{\partial \sigma_x}{\partial x} + \frac{\partial \sigma_{xy}}{\partial y} + \frac{\partial \sigma_{xz}}{\partial z} &= 0 \\ \frac{\partial \sigma_y}{\partial y} + \frac{\partial \sigma_{zy}}{\partial z} + \frac{\partial \sigma_{xy}}{\partial x} &= 0 \\ \frac{\partial \sigma_z}{\partial z} + \frac{\partial \sigma_{xz}}{\partial x} + \frac{\partial \sigma_{yz}}{\partial y} &= 0 . \end{aligned} \quad (11)$$

Consider a differential stress element with the unit normals, as given in Figure 1. The stress vectors on the faces n_x , n_y , and n_z are

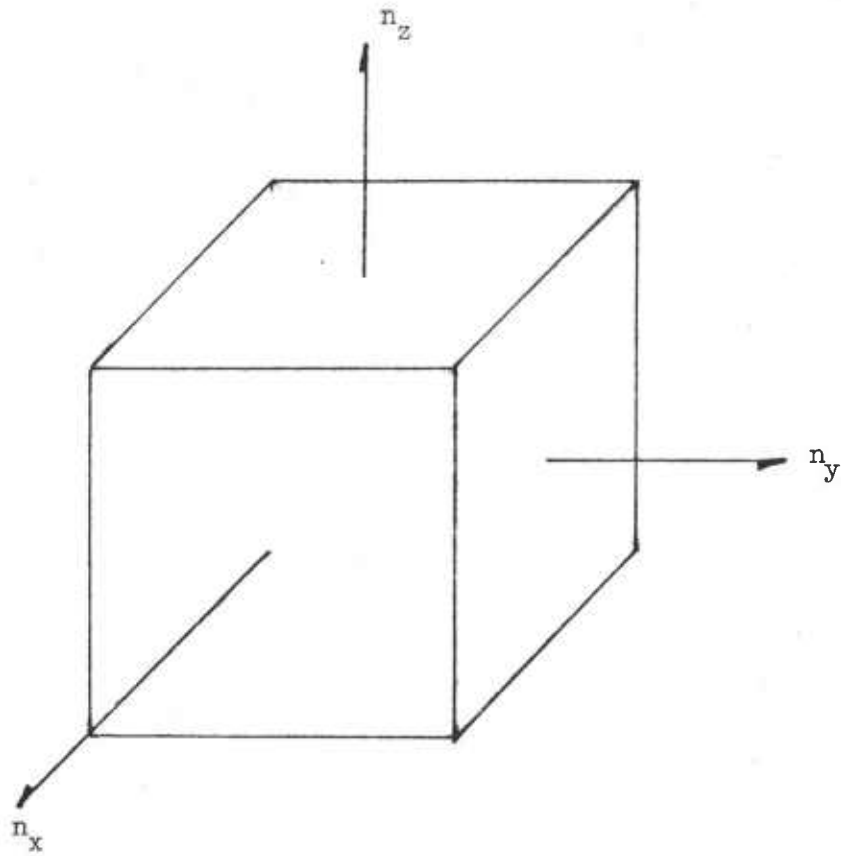


Figure 1. Differential stress element with unit normals n_x, n_y, n_z .

$$\begin{aligned}
\vec{S}_x &= \sigma_{xx} \hat{i} + \sigma_{xy} \hat{j} + \sigma_{xz} \hat{k} \\
\vec{S}_y &= \sigma_{xy} \hat{i} + \sigma_{yy} \hat{j} + \sigma_{yz} \hat{k} \\
\vec{S}_z &= \sigma_{xz} \hat{i} + \sigma_{yz} \hat{j} + \sigma_{zz} \hat{k} \quad ,
\end{aligned} \tag{12}$$

respectively. The equilibrium equations may now be expressed as

$$\begin{aligned}
\vec{\nabla} \cdot \vec{S}_x &= 0 \\
\vec{\nabla} \cdot \vec{S}_y &= 0 \\
\vec{\nabla} \cdot \vec{S}_z &= 0 \quad .
\end{aligned} \tag{13}$$

The stress components may now be written in terms of strain components.
Let

$$G = \frac{E}{2(1 + \mu)} \quad ; \tag{14}$$

$$\begin{aligned}
\text{then } \sigma_x &= 2G \left\{ \frac{\partial u}{\partial x} + \frac{\mu}{1 - 2\mu} \vec{\nabla} \cdot \vec{\rho} \right\} \\
\sigma_y &= 2G \left\{ \frac{\partial v}{\partial y} + \frac{\mu}{1 - 2\mu} \vec{\nabla} \cdot \vec{\rho} \right\} \\
\sigma_z &= 2G \left\{ \frac{\partial w}{\partial z} + \frac{\mu}{1 - 2\mu} \vec{\nabla} \cdot \vec{\rho} \right\} \\
\sigma_{xz} &= G \left\{ \frac{\partial u}{\partial z} + \frac{\partial w}{\partial x} \right\} \\
\sigma_{yz} &= G \left\{ \frac{\partial w}{\partial y} + \frac{\partial v}{\partial z} \right\} \\
\sigma_{xy} &= G \left\{ \frac{\partial u}{\partial y} + \frac{\partial v}{\partial x} \right\} \quad .
\end{aligned} \tag{15}$$

In Eq. (15), $\vec{\rho}$ is the deformation vector between the loaded and unloaded conditions for the solid and is given by

$$\vec{\rho} = u\hat{i} + v\hat{j} + w\hat{k} \quad . \quad (16)$$

Substituting Eq. (15) into Eq. (12) yields

$$\begin{aligned} \vec{S}_x &= G \left(\vec{\nabla}u + \frac{\partial \vec{\rho}}{\partial x} \right) + \hat{i} \frac{2\mu G}{1-2\mu} \vec{\nabla} \cdot \vec{\rho} \\ \vec{S}_y &= G \left(\vec{\nabla}v + \frac{\partial \vec{\rho}}{\partial y} \right) + \hat{j} \frac{2\mu G}{1-2\mu} \vec{\nabla} \cdot \vec{\rho} \\ \vec{S}_z &= G \left(\vec{\nabla}w + \frac{\partial \vec{\rho}}{\partial z} \right) + \hat{k} \frac{2\mu G}{1-2\mu} \vec{\nabla} \cdot \vec{\rho} \quad . \end{aligned} \quad (17)$$

Now, with thermal stress present, a $-\hat{l} \frac{E\alpha\Delta T}{1-2\mu}$ term must be included for each \hat{S}_l stress vector. Therefore,

$$\begin{aligned} \vec{S}_x &= G \left(\vec{\nabla}u + \frac{\partial \vec{\rho}}{\partial x} \right) + \hat{i} \frac{2\mu G}{1-2\mu} \vec{\nabla} \cdot \vec{\rho} - \hat{i} \frac{E\alpha\Delta T}{1-2\mu} \\ \vec{S}_y &= G \left(\vec{\nabla}v + \frac{\partial \vec{\rho}}{\partial y} \right) + \hat{j} \frac{2\mu G}{1-2\mu} \vec{\nabla} \cdot \vec{\rho} - \hat{j} \frac{E\alpha\Delta T}{1-2\mu} \\ \vec{S}_z &= G \left(\vec{\nabla}w + \frac{\partial \vec{\rho}}{\partial z} \right) + \hat{k} \frac{2\mu G}{1-2\mu} \vec{\nabla} \cdot \vec{\rho} - \hat{k} \frac{E\alpha\Delta T}{1-2\mu} \quad . \end{aligned} \quad (18)$$

Now, for equilibrium

$$\begin{aligned}
 \vec{\nabla} \cdot \vec{S}_x &= \vec{\nabla} \cdot G \left(\vec{\nabla} u + \frac{\partial \vec{\rho}}{\partial x} \right) + \vec{\nabla} \cdot \hat{i} \frac{2\mu G}{1-2\mu} \vec{\nabla} \cdot \vec{\rho} - \vec{\nabla} \cdot \hat{i} \frac{E\alpha\Delta T}{1-2\mu} \\
 &= 0 \\
 \vec{\nabla} \cdot \vec{S}_y &= 0 \\
 \vec{\nabla} \cdot \vec{S}_z &= 0 \quad , \quad (19)
 \end{aligned}$$

$$\begin{aligned}
 \text{or } \vec{\nabla} \cdot \vec{S}_x &= G \left\{ \nabla^2 u + \frac{1}{1-2\mu} \frac{\partial}{\partial x} \vec{\nabla} \cdot \vec{\rho} \right\} - \frac{E\alpha}{1-2\mu} \frac{\partial \Delta T}{\partial x} = 0 \\
 \vec{\nabla} \cdot \vec{S}_y &= G \left\{ \nabla^2 v + \frac{1}{1-2\mu} \frac{\partial}{\partial y} \vec{\nabla} \cdot \vec{\rho} \right\} - \frac{E\alpha}{1-2\mu} \frac{\partial \Delta T}{\partial y} = 0 \\
 \vec{\nabla} \cdot \vec{S}_z &= G \left\{ \nabla^2 w + \frac{1}{1-2\mu} \frac{\partial}{\partial z} \vec{\nabla} \cdot \vec{\rho} \right\} - \frac{E\alpha}{1-2\mu} \frac{\partial \Delta T}{\partial z} = 0 \quad ; \quad (20)
 \end{aligned}$$

rearranging terms yields

$$G \left\{ \nabla^2 + \frac{1}{1-2\mu} \vec{\nabla} \vec{\nabla} \cdot \right\} \vec{\rho} = \frac{E\alpha}{1-2\mu} \vec{\nabla} \Delta T \quad ; \quad (21)$$

let

$$\lambda = \frac{E}{(1+\mu)(1-2\mu)} \quad . \quad (22)$$

The deformation vector function $\vec{\rho}$ may now be expressed in terms of the strain potential as

$$2G\vec{\rho} = \vec{\nabla}\phi \quad . \quad (23)$$

Since $\vec{\nabla}\vec{\nabla} \cdot \vec{\nabla} = \vec{\nabla}\vec{\nabla}^2 = \nabla^2\vec{\nabla}$, then Eq. (21) may be written as

$$\begin{aligned} G \left\{ \nabla^2 + \frac{1}{1-2\mu} \vec{\nabla}\vec{\nabla} \cdot \right\} \frac{\vec{\nabla}\phi}{2G} &= \left\{ \nabla^2\vec{\nabla} + \frac{1}{1-2\mu} \nabla^2\vec{\nabla} \right\} \frac{\phi}{2} \\ &= \frac{2-2\mu}{1-2\mu} \vec{\nabla}\nabla^2 \frac{\phi}{2} \\ &= \frac{E\alpha\vec{\nabla}}{1-2\mu} \Delta T \quad , \end{aligned} \quad (24)$$

or

$$\vec{\nabla}\nabla^2 \phi = \frac{E\alpha}{1-\mu} \vec{\nabla}\Delta T \quad ; \quad (25)$$

a sufficient condition is that

$$\nabla^2 \phi = \frac{E\alpha}{1-\mu} \Delta T \quad . \quad (26)$$

Since

$$\begin{aligned} \vec{\rho} &= \frac{\vec{\nabla}\phi}{2G} \\ &= \frac{1}{2G} \left\{ \frac{\partial\phi}{\partial x} \hat{i} + \frac{\partial\phi}{\partial y} \hat{j} + \frac{\partial\phi}{\partial z} \hat{k} \right\} \\ &= u\hat{i} + v\hat{j} + w\hat{k} \quad , \end{aligned} \quad (27)$$

then

$$\sigma_x = \frac{\partial^2 \phi}{\partial x^2} - \nabla^2 \phi$$

$$\sigma_y = \frac{\partial^2 \phi}{\partial y^2} - \nabla^2 \phi$$

$$\sigma_z = \frac{\partial^2 \phi}{\partial z^2} - \nabla^2 \phi ;$$

$$\sigma_{xy} = \frac{\partial^2 \phi}{\partial x \partial y} ;$$

$$\sigma_{yz} = \frac{\partial^2 \phi}{\partial y \partial z} ;$$

$$\sigma_{zx} = \frac{\partial^2 \phi}{\partial z \partial x} . \quad (28)$$

An equivalent expression for Eq. (24) is [2]

$$(\lambda + G) \frac{\partial \varepsilon}{\partial x} + G \nabla^2 u - (3\lambda + 2G) \alpha \frac{\partial \Delta T}{\partial x} = 0$$

$$(\lambda + G) \frac{\partial \varepsilon}{\partial y} + G \nabla^2 v - (3\lambda + 2G) \alpha \frac{\partial \Delta T}{\partial y} = 0$$

$$(\lambda + G) \frac{\partial \varepsilon}{\partial z} + G \nabla^2 w - (3\lambda + 2G) \alpha \frac{\partial \Delta T}{\partial z} = 0 , \quad (29)$$

where ϵ is the dilatation, or

$$\Delta = \frac{\partial u}{\partial x} + \frac{\partial v}{\partial y} + \frac{\partial w}{\partial z} \quad . \quad (30)$$

The relationship between the stress field and temperature change may be expressed as [2]

$$(1 + \mu) \nabla^2 \sigma_x + \frac{\partial^2 I}{\partial x^2} + \alpha E \left\{ \frac{1 + \mu}{1 - \mu} \nabla^2 \Delta T + \frac{\partial^2 \Delta T}{\partial x^2} \right\} = 0$$

$$(1 + \mu) \nabla^2 \sigma_y + \frac{\partial^2 I}{\partial y^2} + \alpha E \left\{ \frac{1 + \mu}{1 - \mu} \nabla^2 \Delta T + \frac{\partial^2 \Delta T}{\partial y^2} \right\} = 0$$

$$(1 + \mu) \nabla^2 \sigma_z + \frac{\partial^2 I}{\partial z^2} + \alpha E \left\{ \frac{1 + \mu}{1 - \mu} \nabla^2 \Delta T + \frac{\partial^2 \Delta T}{\partial z^2} \right\} = 0$$

$$(1 + \mu) \nabla^2 \sigma_{xy} + \frac{\partial^2 I}{\partial x \partial y} + \alpha E \frac{\partial^2 \Delta T}{\partial x \partial y} = 0$$

$$(1 + \mu) \nabla^2 \sigma_{yz} + \frac{\partial^2 I}{\partial y \partial z} + \alpha E \frac{\partial^2 \Delta T}{\partial y \partial z} = 0$$

$$(1 + \mu) \nabla^2 \sigma_{zx} + \frac{\partial^2 I}{\partial z \partial x} + \alpha E \frac{\partial^2 \Delta T}{\partial z \partial x} = 0$$

$$I = \sigma_x + \sigma_y + \sigma_z \quad . \quad (31)$$

B. Laser Speckle Interferometry Theory

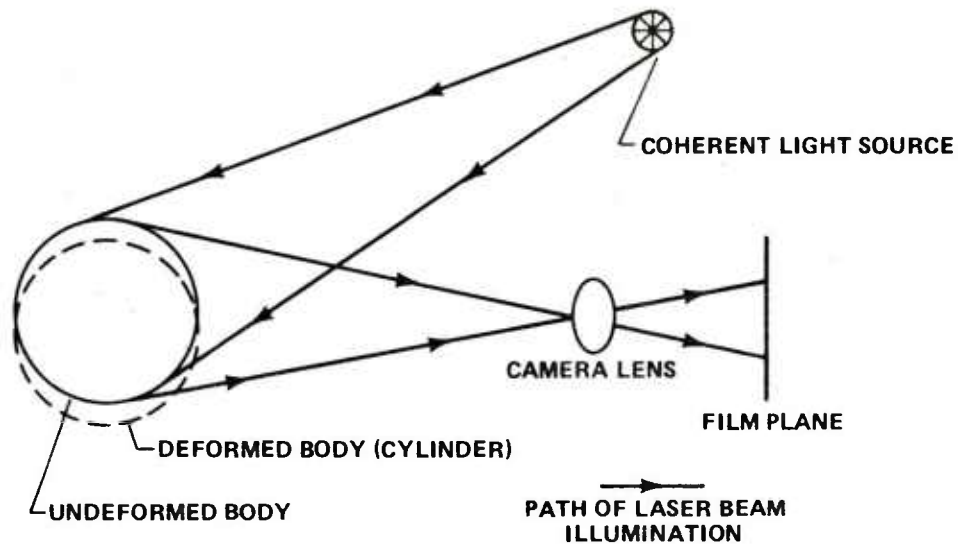
Laser speckle interferograms are most commonly used to make surface displacement measurements of a deformed body. Figure 2 illustrates the basic method for making a laser speckle interferogram. When the diffuse surface of a structure is illuminated with coherent radiation, a grainy speckle effect is imaged by the eye or film plane of a camera due to the interference of light from the structure. This speckle effect is enhanced when the structure has microscopic surface irregularities. If the optical configuration remains fixed, the speckle pattern of the test object may be recorded on the film plane of a camera. Further, if the structure is deformed, the speckle points shift with the deformation and a second exposure of the deformed speckle pattern can be made.

Using a technique of double exposure, speckle interferograms of a structure are normally made by photographing the speckle pattern in a reference and deformed configuration. A beam of laser light is then passed through a region of the double exposure where the local deformation is desired. As the beam passes through the film, the deformed and undeformed speckle recorded there diffract the laser light and cause an interference effect on a viewing screen. A diffraction halo modulated by light and dark bars of light is produced where the distance $2d$ between bars is inversely proportional to the distance between the undeformed and deformed speckle on the film plane. A normal to the light and dark pattern indicates the axis of deformation of the speckle. The theory to be presented assumes that the deformation region illuminated by the laser beam in reconstruction is uniform and that the linear optical theory is applicable.

Figure 3 illustrates the reconstructed diffraction halo modulated by light and dark bars of light. From the linear theory [3], the displacement in the θ direction of a point on the body is given as

$$u_{\theta} = \frac{S\lambda f}{2d} \quad , \quad (32)$$

(A) FORMATION PROCESS



(B) RECONSTRUCTION PROCESS

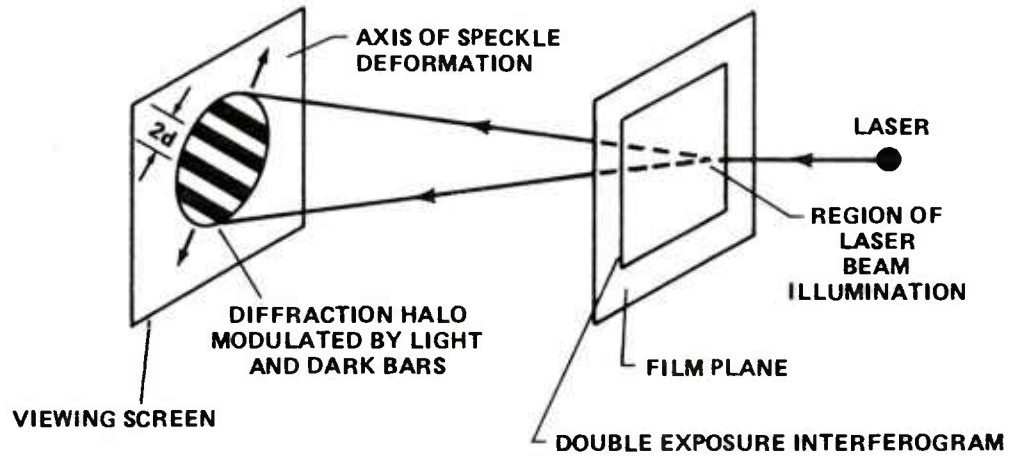


Figure 2. Laser speckle interferometry configuration.

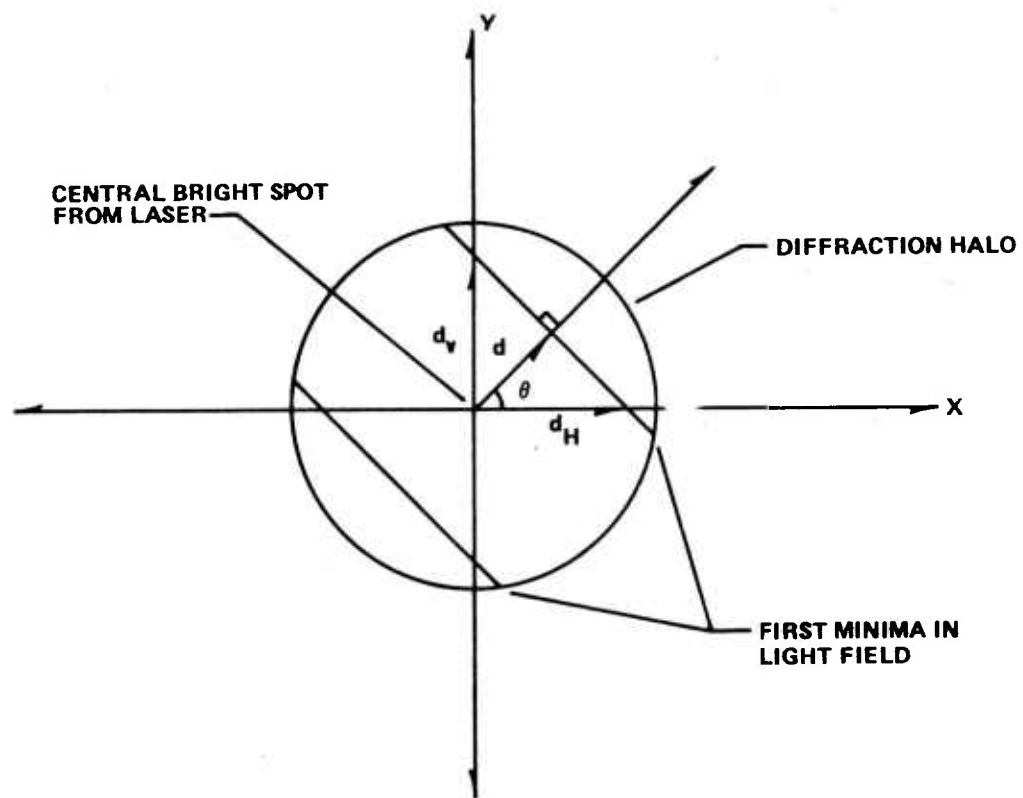


Figure 3. Diffraction halo geometry.

where $S \equiv$ film scale factor (magnification ratio)
 $\lambda \equiv$ wavelength of laser illumination source
 $f \equiv$ distance from interferogram to analyzer screen
 $d \equiv$ distance from central bright spot to first minima
 $U_{\theta} \equiv$ displacement of the point illuminated by the laser on the
 object in the θ direction

The vertical, U_v , and horizontal, U_H , components of displacement may be obtained from U_{θ} as

$$\begin{aligned} U_H &= U_{\theta} \cos \theta = \frac{S\lambda f}{2d} \cos \theta \\ U_v &= U_{\theta} \sin \theta = \frac{S\lambda f}{2d} \sin \theta \end{aligned} \quad (33)$$

and from the geometry

$$\begin{aligned} \frac{d}{d_H} &= \cos \theta \\ \frac{d}{d_v} &= \sin \theta \end{aligned} \quad (34)$$

Therefore,

$$\begin{aligned} U_H &= \frac{S\lambda f}{2d_H} \\ U_v &= \frac{S\lambda f}{2d_v} \end{aligned} \quad (35)$$

Laser speckle interferometry can be used to make very accurate measurements of the in-plane deformation of solids. However, out-of-plane deformation cannot be usefully measured with this technique.

Therefore the technique suffers slightly. In many cases (i.e., thin plates), out-of-plane deformation estimations can be made, which allow accurate measurements of temperature change to be predicted. In a typical application, laser speckle interferometry may be used to estimate the u and v components of deformation, a postulation between the dependence between the w component of deformation and temperature change may be made, and the temperature change of the solid may be estimated based on the simplification of Eq. (29).

C. Thermal Expansion of a Heated Rod

For a uniformly heated rod (Figure 4), the expansion with temperature change may be estimated from

$$\Delta \epsilon = \alpha L \Delta T \quad , \quad (36)$$

where $\Delta \epsilon$ = change in the rod length

α = coefficient of thermal expansion

L = rod length

ΔT = temperature change of rod (uniform)

For a 12-inch rod with a coefficient of thermal expansion equal to $1.66 \times 10^{-5} \text{ } ^\circ\text{C}^{-1}$, a $.502 \text{ } ^\circ\text{C}$ temperature change is required to achieve a $\Delta \epsilon = .0001 \text{ inch}$. Figure 5 illustrates the dependence between $\Delta \epsilon$ and ΔT for various L .

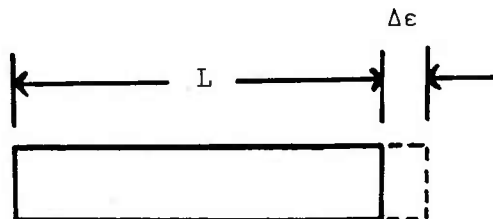


Figure 4. Thermal expansion of a uniformly heated rod.

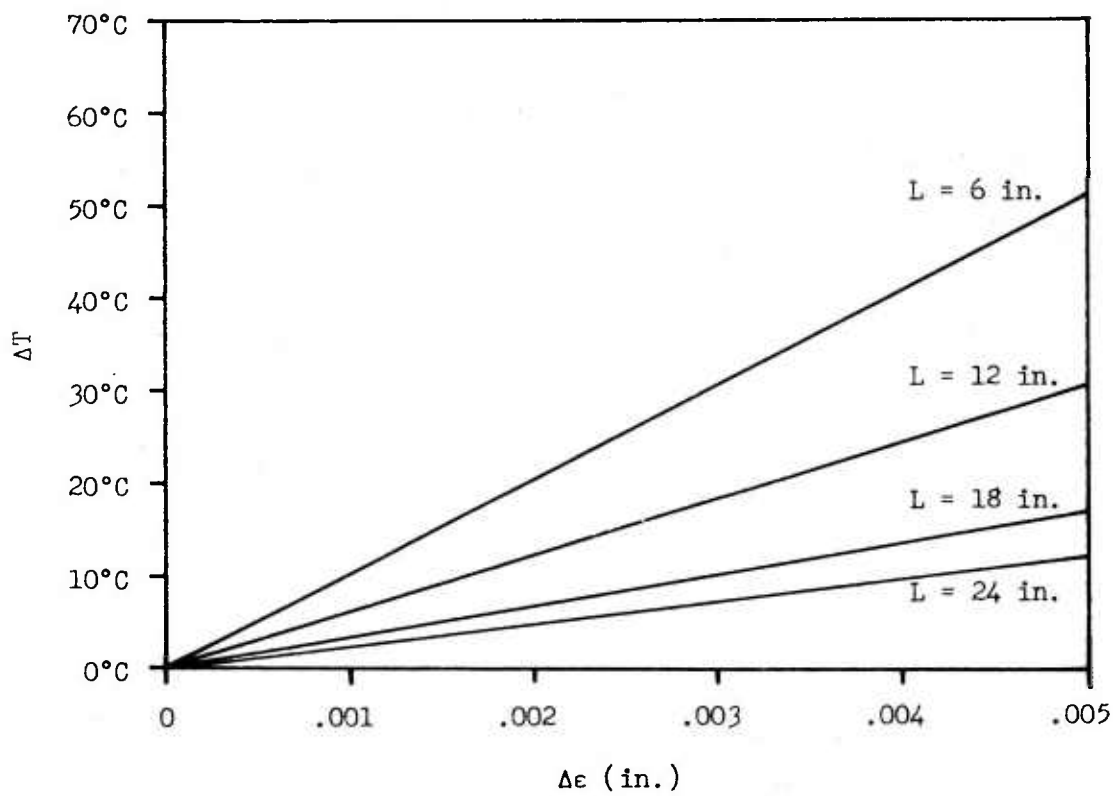


Figure 5. ΔT versus $\Delta \epsilon$ for various rod lengths (L), $\alpha = 1.66 \times 10^{-5} \text{ } ^\circ\text{C}^{-1}$.

D. Thermal Stress Deformation of a Thin Circular Plate Neglecting the z Component of Deformation

The general temperature/deformation equations take the form

$$\begin{aligned}\nabla^2 \phi &= \frac{E\alpha}{1-\mu} \Delta T \\ \frac{\vec{\nabla} \phi}{\rho} &= \frac{\vec{\nabla} \phi}{2G}\end{aligned}\quad (37)$$

The Laplacian and Gradient in cylindrical coordinates are

$$\begin{aligned}\nabla^2 \phi &= \frac{1}{r} \frac{\partial}{\partial r} \left\{ r \frac{\partial \phi}{\partial r} \right\} + \frac{1}{r^2} \frac{\partial^2 \phi}{\partial \theta^2} + \frac{\partial^2 \phi}{\partial z^2} \\ \vec{\nabla} \phi &= \frac{\partial \phi}{\partial r} \hat{e}_r + \frac{1}{r} \frac{\partial \phi}{\partial \theta} \hat{e}_\theta + \frac{\partial \phi}{\partial z} \hat{e}_z\end{aligned}\quad (38)$$

For a circular plate with a radial temperature distribution $\Delta T = \Delta T(r)$ and neglecting the z component of plate deformation,

$$\begin{aligned}\frac{1}{r} \frac{\partial}{\partial r} \left\{ r \frac{\partial \phi}{\partial r} \right\} &= \frac{E\alpha}{1-\mu} \Delta T \\ \phi &= \phi(r) \text{ only.}\end{aligned}\quad (39)$$

For such a symmetric circular plate,

$$\vec{\nabla} \phi = \frac{\partial \phi}{\partial r} \hat{e}_r \quad (40)$$

Therefore,

$$\frac{1}{r} \frac{\partial}{\partial r} \left\{ r \frac{\partial \phi}{\partial r} \right\} = \frac{E\alpha}{1-\mu} \Delta T$$

$$\frac{\partial}{\partial r} \left\{ r \frac{\partial \phi}{\partial r} \right\} = \frac{rE\alpha}{1-\mu} \Delta T$$

$$r \frac{\partial \phi}{\partial r} = \int_0^r \frac{rE\alpha}{1-\mu} \Delta T \, dr + C_1$$

$$\frac{\partial \phi}{\partial r} = \frac{1}{r} \int_0^r \frac{rE\alpha}{1-\mu} \Delta T \, dr + \frac{C_1}{r}$$

$$C_1 = 0 \quad \text{since } \frac{\partial \phi}{\partial r} = 0 \text{ at } r = 0$$

$$\frac{\partial \phi}{\partial r} = \frac{1}{2G} \frac{\partial \phi}{\partial r} \hat{e}_r \quad (41)$$

and

$$\frac{\partial \phi}{\partial r} = \left\{ \frac{1}{2Gr} \int_0^r \frac{rE\alpha}{1-\mu} \Delta T \, dr \hat{e}_r \right\} \quad (42)$$

The radial deformation measured with laser speckle interferometry may be expressed as

$$\rho_r \hat{e}_r = \frac{m\lambda f S}{\chi(r)} \hat{e}_r \quad , \quad (43)$$

where $S \equiv$ film scale factor
 $f \equiv$ viewing screen to interferogram distance
 $\lambda \equiv$ light source wavelength
 $m \equiv$ fringe order
 $\chi(r) \equiv$ fringe spacing

Substituting Eq. (43) into Eq. (42),

$$\frac{m\lambda f S}{\chi(r)} \hat{e}_r = \frac{1}{2Gr} \int_0^r \frac{rE\alpha}{1-\mu} \Delta T dr \hat{e}_r, \quad (44)$$

or

$$\begin{aligned} \chi(r) &= \left\{ \frac{1}{2Gm\lambda fSr} \int_0^r \frac{rE\alpha}{1-\mu} \Delta T dr \right\}^{-1} \\ \chi(r) &= \frac{2 \left\{ \frac{E}{2(1+\mu)} \right\} m\lambda fSr}{\left\{ \frac{E}{1-\mu} \right\} \int_0^r r \Delta T dr} \\ \chi(r) &= \frac{\left\{ \frac{1-\mu}{1+\mu} \right\} m\lambda fSr}{\alpha \int_0^r r \Delta T(r) dr}. \end{aligned} \quad (45)$$

For laboratory analysis, $\chi(r)$ is measured as the first minima to first minima spacing; i.e., $m = 1$. Therefore,

$$\chi(r) = \frac{\left\{ \frac{1-\mu}{1+\mu} \right\} \lambda fSr}{\alpha \int_0^r r \Delta T(r) dr}. \quad (46)$$

E. Thermal Stress Deformation of a Thin Circular Plate with a Correction for the z Component of Deformation

Consider a thin circular plate as shown in Figure 6. The potential function for this case is $\phi = f(r, z)$; therefore

$$\vec{\rho} = \frac{1}{2G} \vec{\nabla} \phi = \frac{1}{2G} \left\{ \frac{\partial \phi}{\partial r} \hat{e}_r + \frac{\partial \phi}{\partial z} \hat{e}_z \right\}, \quad (47)$$

and

$$\begin{aligned} \frac{1}{r} \frac{\partial \phi}{\partial r} \left\{ r \frac{\partial \phi}{\partial r} \right\} + \frac{\partial^2 \phi}{\partial z^2} &= \frac{E\alpha}{1-\mu} \Delta T \\ \frac{1}{r} \frac{\partial \phi}{\partial r} + \frac{\partial^2 \phi}{\partial r^2} + \frac{\partial^2 \phi}{\partial z^2} &= \frac{E\alpha}{1-\mu} \Delta T \end{aligned} \quad (48)$$

To simplify, let

$$\Delta T = \Delta T(r);$$

thus

$$\frac{1}{r} \frac{\partial \phi}{\partial r} + \frac{\partial^2 \phi}{\partial r^2} + \frac{\partial^2 \phi}{\partial z^2} = \frac{E\alpha}{1-\mu} \Delta T(r), \quad (49)$$

and

$$\vec{\rho} = \frac{\vec{\nabla} \phi}{2G} = \frac{1}{2G} \left\{ \frac{\partial \phi}{\partial r} \hat{e}_r + \frac{\partial \phi}{\partial z} \hat{e}_z \right\} = \frac{m\lambda f S}{\chi(r)} \hat{e}_r + \frac{\partial \phi}{2G \partial z} \hat{e}_z, \quad (50)$$

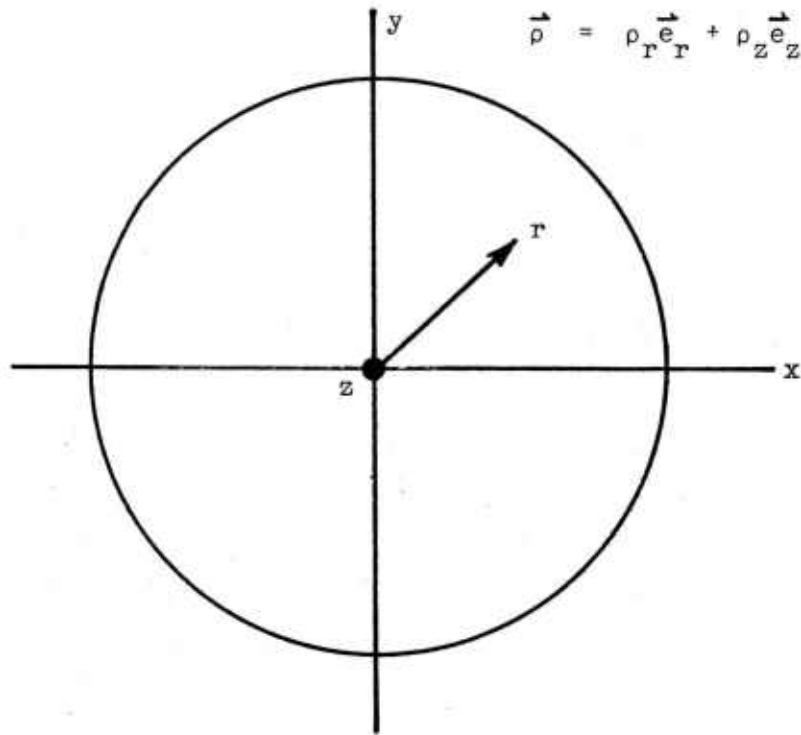


Figure 6. Thermal stress deformation of a thin circular plate with ρ_r and ρ_z components of deformation.

or

$$\frac{1}{2G} \frac{\partial \phi}{\partial r} = \frac{m\lambda f S}{\chi(r)}$$

$$\frac{\partial \phi}{\partial r} = \frac{2Gm\lambda f S}{\chi(r)} \quad (51)$$

The thermal profile equation then takes the form

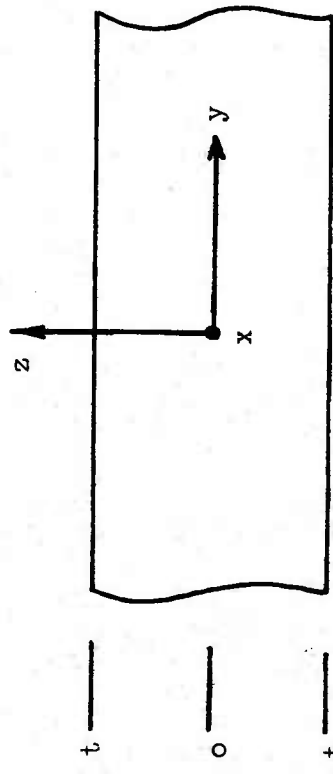
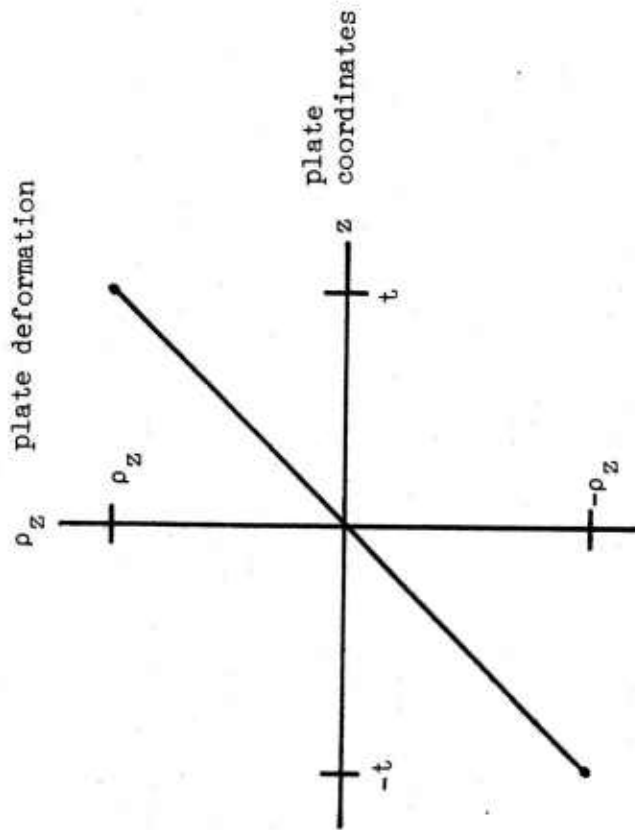
$$\frac{1}{r} \frac{2Gm\lambda f S}{\chi(r)} + 2Gm\lambda f S \frac{\partial}{\partial r} \left\{ \frac{1}{\chi(r)} \right\} + \frac{\partial^2 \phi}{\partial z^2} = \frac{E\alpha}{1-\mu} \Delta T(r) \quad (52)$$

With laser speckle interferometry, the \hat{e}_z component of displacement cannot be measured. Only an estimate of the significance of $\partial^2 \phi / \partial z^2$ in the thermal profile equation can be made. Assume that the plate is of thickness $2t$, which is thin enough that there is no temperature variation in the z direction. Figure 7 illustrates the assumed deformation profile. From this figure, the deformation is linear with z and takes the form

$$\vec{\rho}_z = \alpha \Delta T z \hat{e}_z = \frac{1}{2G} \frac{\partial \phi}{\partial z} \hat{e}_z$$

$$\frac{\partial \phi}{\partial z} = 2G\alpha \Delta T z$$

$$\frac{\partial^2 \phi}{\partial z^2} = 2G\alpha \Delta T \quad (53)$$



The plate thickness = $2t$

$$\rho_z = \alpha z \Delta T$$

ΔT = temperature change

Figure 7. Assumed deformation profile in the z direction of a heated flat plate.

Substituting Eq. (53) into Eq. (52) yields

$$\frac{1}{r} 2G \frac{m\lambda fS}{\chi(r)} + 2Gm\lambda fS \frac{\partial}{\partial r} \left\{ \frac{1}{\chi(r)} \right\} + 2G\alpha \Delta T(r) = \frac{E\alpha}{1-\mu} \Delta T(r)$$

and

$$\Delta T(r) \left\{ \frac{E\alpha}{1-\mu} - 2G\alpha \right\} = 2Gm\lambda fS \left\{ \frac{1}{r} \frac{1}{\chi(r)} + \frac{\partial}{\partial r} \frac{1}{\chi(r)} \right\} \quad (54)$$

Define

$$D(r) = \left\{ \frac{1}{r} \frac{1}{\chi(r)} + \frac{\partial}{\partial r} \left\{ \frac{1}{\chi(r)} \right\} \right\}$$

$$\beta = \frac{m\lambda fS}{2\alpha} \left\{ \frac{1-\mu}{\mu} \right\} ; \quad (55)$$

then

$$\Delta T(r) = \beta D(r) \quad (56)$$

Let

$$\gamma(r) = \frac{r}{\chi(r)} , \quad (57)$$

then

$$\Delta T(r) = \frac{\beta}{r} \frac{\partial \gamma(r)}{\partial r} \quad (58)$$

F. Thin Plate Thermostress Equations in Rectangular Coordinates

In rectangular coordinates,

$$2G\vec{\rho} = \vec{\nabla}\phi = \frac{\partial\phi}{\partial x}\hat{e}_x + \frac{\partial\phi}{\partial y}\hat{e}_y + \frac{\partial\phi}{\partial z}\hat{e}_z$$

$$\nabla^2\phi = \frac{E\alpha}{1-\mu}\Delta T = \frac{\partial^2\phi}{\partial x^2} + \frac{\partial^2\phi}{\partial y^2} + \frac{\partial^2\phi}{\partial z^2} \quad (59)$$

By substituting,

$$\frac{\partial}{\partial x}(2G\rho_x) + \frac{\partial}{\partial y}(2G\rho_y) + \frac{\partial}{\partial z}(2G\rho_z) = \frac{E\alpha}{1-\mu}\Delta T$$

$$\frac{\partial\rho_x}{\partial x} + \frac{\partial\rho_y}{\partial y} + \frac{\partial\rho_z}{\partial z} = \alpha \left\{ \frac{1+\mu}{1-\mu} \right\} \Delta T \quad (60)$$

In general,

$$\Delta T = \frac{1}{\alpha} \left\{ \frac{1-\mu}{1+\mu} \right\} \left\{ \frac{\partial\rho_x}{\partial x} + \frac{\partial\rho_y}{\partial y} + \frac{\partial\rho_z}{\partial z} \right\} \quad (61)$$

For thin plates, there are two independent approximations:

$$1. \quad \rho_z = \alpha\Delta Tz$$

$$\frac{\partial\rho_z}{\partial z} = \alpha\Delta T$$

$$2. \quad \frac{\partial\rho_z}{\partial z} \approx 0$$

It is important to note that in many instances, Eq. (61) will not satisfy all the boundary conditions of a problem. For approximation 1,

$$\Delta T = \frac{1}{\alpha} \left\{ \frac{1-\mu}{1+\mu} \right\} \left\{ \frac{\partial \rho_x}{\partial x} + \frac{\partial \rho_y}{\partial y} \right\} + \left\{ \frac{1-\mu}{1+\mu} \right\} \Delta T \quad (62)$$

Let

$$\psi_1 = \frac{\frac{1}{\alpha} \left\{ \frac{1-\mu}{1+\mu} \right\}}{1 - \left\{ \frac{1-\mu}{1+\mu} \right\}} \quad (63)$$

Therefore

$$\Delta T = \psi_1 \left\{ \frac{\partial \rho_x}{\partial x} + \frac{\partial \rho_y}{\partial y} \right\} \quad (64)$$

For approximation 2, let

$$\psi_2 = \frac{1}{\alpha} \left\{ \frac{1-\mu}{1+\mu} \right\} \quad (65)$$

then

$$\Delta T = \psi_2 \left\{ \frac{\partial \rho_x}{\partial x} + \frac{\partial \rho_y}{\partial y} \right\} \quad (66)$$

Using laser speckle interferometry, approximation 1 may be expressed as

$$\Delta T = \frac{\psi_1 S \lambda f}{2} \left\{ \frac{\partial}{\partial x} \left(\frac{1}{d_H} \right) + \frac{\partial}{\partial y} \left(\frac{1}{d_V} \right) \right\} \quad (67)$$

and approximation 2 is

$$\Delta T = \frac{\psi_2 S \lambda f}{2} \left\{ \frac{\partial}{\partial x} \left(\frac{1}{d_H} \right) + \frac{\partial}{\partial y} \left(\frac{1}{d_V} \right) \right\} \quad (68)$$

G. Numerical Differentiation of the Thermal Induced Deformation Field to Predict Temperature Change

Suppose the temperature change upon heating or cooling is desired at some location i, j on a body. The x components U_{i-1} , U_i , U_{i+1} and the y components V_{j-1} , V_j , V_{j+1} of displacement have been determined. Figure 8 illustrates the geometry.

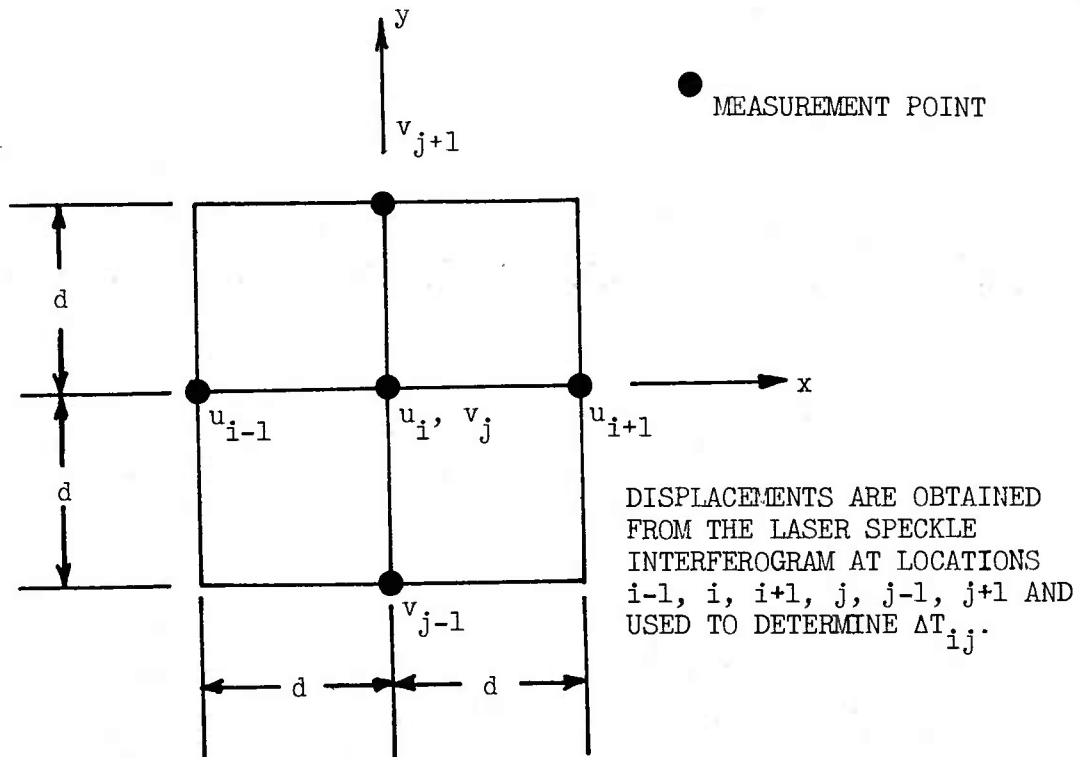


Figure 8. Geometry for measuring temperature change ΔT at location i, j .

The approximation to the derivative

$$\rho(x,y) = \frac{\partial \rho}{\partial x} x + \frac{\partial \rho}{\partial y} y \quad (69)$$

may be obtained as follows:

$$\frac{\partial \rho}{\partial x} \approx \frac{1}{2} \left\{ \frac{U_i - U_{i-1}}{d} + \frac{U_{i+1} - U_i}{d} \right\} = \frac{U_{i+1} - U_{i-1}}{2d}$$

$$\frac{\partial \rho}{\partial y} \approx \frac{1}{2} \left\{ \frac{V_j - V_{j-1}}{d} + \frac{V_{j+1} - V_j}{d} \right\} = \frac{V_{j+1} - V_{j-1}}{2d}$$

or

$$\rho(x,y) \approx \frac{U_{i+1} - U_{i-1} + V_{j+1} - V_{j-1}}{2d} \quad (70)$$

Using laser speckle interferometry,

$$\rho(x,y) = \frac{S\lambda f}{4d} \left\{ \frac{1}{d_{H_{i+1}}} - \frac{1}{d_{H_{i-1}}} + \frac{1}{d_{V_{j+1}}} - \frac{1}{d_{V_{j-1}}} \right\} \quad (71)$$

H. Deformation of Circular Flat Plates in Cylindrical Coordinates

The following set of equations are derived in cylindrical coordinates to relate the change of temperature field in thin circular flat plates to the corresponding deformation field. For cylindrical coordinates,

$$G \left\{ \nabla^2 + \frac{1}{1-2\mu} \vec{\nabla} \vec{\nabla} \cdot \right\} \frac{\vec{\nabla} \phi}{2G} = \left\{ \frac{E\alpha}{1-2\mu} \right\} \vec{\nabla} \Delta T \quad (72)$$

$$\vec{\nabla} \phi = \frac{\partial \phi}{\partial r} \hat{e}_r + \frac{1}{r} \frac{\partial \phi}{\partial \theta} \hat{e}_\theta + \frac{\partial \phi}{\partial z} \hat{e}_z \quad (73)$$

$$\nabla^2 \phi = \frac{1}{r} \frac{\partial}{\partial r} \left\{ r \frac{\partial \phi}{\partial r} \right\} + \frac{1}{r^2} \frac{\partial^2 \phi}{\partial \theta^2} + \frac{\partial^2 \phi}{\partial z^2} \quad (74)$$

$$\vec{\nabla} \cdot \vec{\phi} = \frac{1}{r} \frac{\partial}{\partial r} (r \phi_r) + \frac{1}{r} \frac{\partial}{\partial \theta} (\phi_\theta) + \frac{\partial}{\partial z} (\phi_z) \quad (75)$$

The derivatives of the cylindrical vectors \hat{e}_θ and \hat{e}_r are [4]

$$\frac{\partial}{\partial \theta} \hat{e}_\theta = -\hat{e}_r \quad (76)$$

$$\frac{\partial}{\partial \theta} \hat{e}_r = \hat{e}_\theta \quad (77)$$

Since

$$\frac{1}{\rho} = \frac{\vec{\nabla} \phi}{2G}, \quad (78)$$

then

$$G \left\{ \nabla^2 + \frac{1}{1-2\mu} \vec{\nabla} \vec{\nabla} \cdot \right\} \frac{1}{\rho} = \left\{ \frac{E\alpha}{1-2\mu} \right\} \vec{\nabla} \Delta T \quad (79)$$

$$\left\{ \nabla^2 + \frac{1}{1-2\mu} \vec{\nabla} \vec{\nabla} \cdot \right\} \frac{1}{\rho} = \frac{2(1+\mu)\alpha}{1-2\mu} \vec{\nabla} \Delta T \quad (80)$$

Let

$$\gamma = \frac{1}{1 - 2\mu} \quad (81)$$

$$\beta = \frac{2(1 + \mu)}{1 - 2\mu} \quad (82)$$

Now Eq. (80) may be written as

$$\left\{ \nabla^2 + \gamma \vec{\nabla} \vec{\nabla} \cdot \right\} \vec{\rho} = \beta \vec{\nabla} \Delta T \quad (83)$$

Expanding Eq. (83),

$$\begin{aligned} & \left(\frac{1}{r} \frac{\partial}{\partial r} \left\{ r \frac{\partial}{\partial r} \right\} + \frac{1}{r^2} \frac{\partial^2}{\partial \theta^2} + \frac{\partial^2}{\partial z^2} \right) (\rho_r \hat{e}_r + \rho_\theta \hat{e}_\theta + \rho_z \hat{e}_z) \\ & + \gamma \left(\frac{\partial}{\partial r} \hat{e}_r + \frac{1}{r} \frac{\partial}{\partial \theta} \hat{e}_\theta + \frac{\partial}{\partial z} \hat{e}_z \right) \left(\frac{\partial}{\partial r} \hat{e}_r + \frac{1}{r} \frac{\partial}{\partial \theta} \hat{e}_\theta + \frac{\partial}{\partial z} \hat{e}_z \right) \\ & \cdot (\rho_r \hat{e}_r + \rho_\theta \hat{e}_\theta + \rho_z \hat{e}_z) = \beta \left(\frac{\partial}{\partial r} \hat{e}_r + \frac{1}{r} \frac{\partial}{\partial \theta} \hat{e}_\theta + \frac{\partial}{\partial z} \hat{e}_z \right) \Delta T \quad (84) \end{aligned}$$

Further expansion yields

$$\begin{aligned}
& \frac{1}{r} \frac{\partial}{\partial r} \left\{ r \frac{\partial}{\partial r} (\rho_r \hat{e}_r) \right\} + \frac{1}{r} \frac{\partial}{\partial r} \left\{ r \frac{\partial}{\partial r} (\rho_\theta \hat{e}_\theta) \right\} + \frac{1}{r} \frac{\partial}{\partial r} \left\{ r \frac{\partial}{\partial r} (\rho_z \hat{e}_z) \right\} \\
& + \frac{1}{r^2} \frac{\partial^2}{\partial \theta^2} (\rho_r \hat{e}_r) + \frac{1}{r^2} \frac{\partial^2}{\partial \theta^2} (\rho_\theta \hat{e}_\theta) + \frac{1}{r^2} \frac{\partial^2}{\partial \theta^2} (\rho_z \hat{e}_z) \\
& + \frac{\partial^2}{\partial z^2} (\rho_r \hat{e}_r) + \frac{\partial^2}{\partial z^2} (\rho_\theta \hat{e}_\theta) + \frac{\partial^2}{\partial z^2} (\rho_z \hat{e}_z) \\
& + \gamma \left\{ \frac{\partial}{\partial r} \hat{e}_r + \frac{1}{r} \frac{\partial}{\partial \theta} \hat{e}_\theta + \frac{\partial}{\partial z} \hat{e}_z \right\} \left\{ \frac{1}{r} \frac{\partial}{\partial r} (r \rho_r) + \frac{1}{r} \frac{\partial}{\partial \theta} \rho_\theta \right. \\
& \quad \left. + \frac{\partial}{\partial z} \rho_z \right\} = \beta \left\{ \frac{\partial \Delta T}{\partial r} \hat{e}_r + \frac{1}{r} \frac{\partial \Delta T}{\partial \theta} \hat{e}_\theta + \frac{\partial \Delta T}{\partial z} \hat{e}_z \right\} \quad (85)
\end{aligned}$$

In cylindrical coordinates,

$$\frac{\partial}{\partial \theta} (\rho_r \hat{e}_r) = \frac{\partial \rho_r}{\partial \theta} \hat{e}_r + \rho_r \hat{e}_\theta \quad (86)$$

$$\frac{\partial^2}{\partial \theta^2} (\rho_r \hat{e}_r) = \frac{\partial^2 \rho_r}{\partial \theta^2} \hat{e}_r + \frac{\partial \rho_r}{\partial \theta} \hat{e}_\theta + \frac{\partial \rho_r}{\partial \theta} \hat{e}_\theta - \rho_r \hat{e}_r \quad (87)$$

$$\frac{\partial}{\partial \theta} (\rho_\theta \hat{e}_\theta) = \frac{\partial \rho_\theta}{\partial \theta} \hat{e}_\theta - \rho_\theta \hat{e}_r \quad (88)$$

$$\frac{\partial^2}{\partial \theta^2} (\rho_\theta \hat{e}_\theta) = \frac{\partial^2 \rho_\theta}{\partial \theta^2} \hat{e}_\theta - \frac{\partial \rho_\theta}{\partial \theta} \hat{e}_r - \frac{\partial \rho_\theta}{\partial \theta} \hat{e}_r - \rho_\theta \hat{e}_\theta \quad (89)$$

Substituting Eqs. (86), (87), (88), and (89) into Eq. (85) yields

$$\begin{aligned}
& \frac{1}{r} \frac{\partial}{\partial r} \left\{ r \frac{\partial \rho_r}{\partial r} \right\} \hat{e}_r + \frac{1}{r} \frac{\partial}{\partial r} \left\{ r \frac{\partial}{\partial r} (\rho_\theta \hat{e}_\theta) \right\} + \frac{1}{r} \frac{\partial}{\partial r} \left\{ r \frac{\partial \rho_z}{\partial r} \right\} \hat{e}_z \\
& + \frac{1}{r^2} \frac{\partial^2 \rho_r}{\partial \theta^2} \hat{e}_r + \frac{2}{r^2} \frac{\partial \rho_r}{\partial \theta} \hat{e}_\theta - \frac{\rho_r}{r^2} \hat{e}_r \\
& + \frac{1}{r^2} \frac{\partial^2 \rho_\theta}{\partial \theta^2} \hat{e}_\theta - \frac{2}{r^2} \frac{\partial \rho_\theta}{\partial \theta} \hat{e}_r - \frac{\rho_\theta}{r^2} \hat{e}_\theta \\
& + \frac{1}{r^2} \frac{\partial^2 \rho_z}{\partial \theta^2} \hat{e}_z + \frac{\partial^2 \rho_r}{\partial z^2} \hat{e}_r + \frac{\partial^2 \rho_\theta}{\partial z^2} \hat{e}_\theta \\
& + \frac{\partial^2 \rho_z}{\partial z^2} \hat{e}_z + \gamma \frac{\partial}{\partial r} \left\{ \frac{1}{r} \frac{\partial}{\partial r} (r \rho_r) + \frac{1}{r} \frac{\partial}{\partial \theta} \rho_\theta + \frac{\partial}{\partial z} \rho_z \right\} \hat{e}_r \\
& + \gamma \frac{\partial}{\partial \theta} \left\{ \frac{1}{r} \frac{\partial}{\partial r} (r \rho_r) + \frac{1}{r} \frac{\partial}{\partial \theta} \rho_\theta + \frac{\partial}{\partial z} \rho_z \right\} \hat{e}_\theta \\
& + \gamma \frac{\partial}{\partial z} \left\{ \frac{1}{r} \frac{\partial}{\partial r} (r \rho_r) + \frac{1}{r} \frac{\partial}{\partial \theta} \rho_\theta + \frac{\partial}{\partial z} \rho_z \right\} \hat{e}_z \\
& = \beta \left\{ \frac{\partial \Delta T}{\partial r} \hat{e}_r + \frac{1}{r} \frac{\partial \Delta T}{\partial \theta} \hat{e}_\theta + \frac{\partial \Delta T}{\partial z} \hat{e}_z \right\} \quad (90)
\end{aligned}$$

Assume for the cylindrical plate that due to symmetry, $\rho_\theta = 0$.
Therefore,

$$\begin{aligned}
& \frac{1}{r} \frac{\partial}{\partial r} \left\{ r \frac{\partial \rho_r}{\partial r} \right\} \hat{e}_r + \frac{1}{r} \frac{\partial}{\partial r} \left\{ r \frac{\partial \rho_z}{\partial r} \right\} \hat{e}_z + \frac{1}{r^2} \frac{\partial^2 \rho_r}{\partial \theta^2} \hat{e}_r + \frac{2}{r^2} \frac{\partial \rho_r}{\partial \theta} \hat{e}_\theta \\
& - \frac{\rho_r}{r^2} \hat{e}_r + \frac{1}{r^2} \frac{\partial^2 \rho_z}{\partial \theta^2} \hat{e}_z + \frac{\partial^2 \rho_r}{\partial z^2} \hat{e}_r + \frac{\partial^2 \rho_z}{\partial z^2} \hat{e}_z \\
& + \gamma \frac{\partial}{\partial r} \left\{ \frac{1}{r} \frac{\partial}{\partial r} (r \rho_r) + \frac{\partial}{\partial z} \rho_z \right\} \hat{e}_r \\
& + \gamma \frac{\partial}{\partial \theta} \left\{ \frac{1}{r} \frac{\partial}{\partial r} (r \rho_r) + \frac{\partial \rho_z}{\partial z} \right\} \hat{e}_\theta \\
& + \gamma \frac{\partial}{\partial z} \left\{ \frac{1}{r} \frac{\partial}{\partial r} (r \rho_r) + \frac{\partial \rho_z}{\partial z} \right\} \hat{e}_z \\
& = \beta \left\{ \frac{\partial \Delta T}{\partial r} \hat{e}_r + \frac{1}{r} \frac{\partial \Delta T}{\partial \theta} \hat{e}_\theta + \frac{\partial \Delta T}{\partial z} \hat{e}_z \right\} \quad . \quad (91)
\end{aligned}$$

Assume that $\rho_r = \rho_r(r)$ and $\rho_z = \rho_z(r, z)$; then

$$\begin{aligned}
& \frac{1}{r} \frac{\partial}{\partial r} \left\{ r \frac{\partial \rho_r}{\partial r} \right\} \hat{e}_r + \frac{1}{r} \frac{\partial}{\partial r} \left\{ r \frac{\partial \rho_z}{\partial r} \right\} \hat{e}_z - \frac{\rho_r}{r^2} \hat{e}_r + \frac{\partial^2 \rho_z}{\partial z^2} \hat{e}_z \\
& + \gamma \frac{\partial}{\partial r} \left\{ \frac{1}{r} \frac{\partial}{\partial r} (r \rho_r) + \frac{\partial \rho_z}{\partial z} \right\} \hat{e}_r \\
& + \gamma \frac{\partial}{\partial z} \left\{ \frac{1}{r} \frac{\partial}{\partial r} (r \rho_r) + \frac{\partial \rho_z}{\partial z} \right\} \hat{e}_z \\
& = \beta \left\{ \frac{\partial \Delta T}{\partial r} \hat{e}_r + \frac{1}{r} \frac{\partial \Delta T}{\partial \theta} \hat{e}_\theta + \frac{\partial \Delta T}{\partial z} \hat{e}_z \right\} \quad . \quad (92)
\end{aligned}$$

From Eq. (92),

$$\frac{\partial \Delta T}{\partial \theta} = 0 \quad (93)$$

Examine the \hat{e}_r variation in Eq. (92);

$$\frac{1}{r} \frac{\partial}{\partial r} \left\{ r \frac{\partial \rho_r}{\partial r} \right\} \hat{e}_r - \frac{\rho_r \hat{e}_r}{r^2} + \gamma \frac{\partial}{\partial r} \left\{ \frac{1}{r} \frac{\partial}{\partial r} (r \rho_r) + \frac{\partial \rho_z}{\partial z} \right\} \hat{e}_r = \beta \frac{\partial \Delta T}{\partial r} \hat{e}_r \quad (94)$$

or

$$\frac{1}{r} \frac{\partial}{\partial r} \left\{ r \frac{\partial \rho_r}{\partial r} \right\} - \frac{\rho_r}{r^2} + \gamma \frac{\partial}{\partial r} \left\{ \frac{1}{r} \frac{\partial}{\partial r} (r \rho_r) + \frac{\partial \rho_z}{\partial z} \right\} = \beta \frac{\partial \Delta T}{\partial r} \quad (95)$$

Expanding Eq. (95),

$$\frac{\partial^2 \rho_r}{\partial r^2} + \frac{1}{r} \frac{\partial \rho_r}{\partial r} - \frac{\rho_r}{r^2} + \gamma \frac{\partial}{\partial r} \left\{ \frac{\partial \rho_r}{\partial r} + \frac{\rho_r}{r} \right\} + \gamma \frac{\partial^2 \rho_z}{\partial r \partial z} = \beta \frac{\partial \Delta T}{\partial r} \quad (96)$$

$$\frac{\partial^2 \rho_r}{\partial r^2} + \frac{1}{r} \frac{\partial \rho_r}{\partial r} - \frac{\rho_r}{r^2} + \gamma \frac{\partial^2 \rho_r}{\partial r^2} + \frac{\gamma}{r} \frac{\partial \rho_r}{\partial r} - \gamma \frac{\rho_r}{r^2} + \gamma \frac{\partial^2 \rho_z}{\partial r \partial z} = \beta \frac{\partial \Delta T}{\partial r} \quad (97)$$

$$(1 + \gamma) \frac{\partial^2 \rho_r}{\partial r^2} + (1 + \gamma) \frac{1}{r} \frac{\partial \rho_r}{\partial r} - (1 + \gamma) \frac{\rho_r}{r^2} + \gamma \frac{\partial^2 \rho_z}{\partial r \partial z} = \beta \frac{\partial \Delta T}{\partial r} \quad (98)$$

$$(1 + \gamma) \left\{ \frac{\partial^2 \rho_r}{\partial r^2} + \frac{1}{r} \frac{\partial \rho_r}{\partial r} - \frac{\rho_r}{r^2} \right\} + \gamma \frac{\partial^2 \rho_z}{\partial r \partial z} = \beta \frac{\partial \Delta T}{\partial r} \quad (99)$$

In general, assume $\rho_z = \alpha z \Delta T(r)$. Then

$$\gamma \frac{\partial^2 \rho_z}{\partial r \partial z} = \gamma \frac{\partial}{\partial r} (\alpha \Delta T) = \gamma \alpha \frac{\partial \Delta T}{\partial r}, \quad (100)$$

and

$$(1 + \gamma) \left\{ \frac{\partial^2 \rho_r}{\partial r^2} + \frac{1}{r} \frac{\partial \rho_r}{\partial r} - \frac{\rho_r}{r^2} \right\} = (\beta - \alpha \gamma) \frac{\partial \Delta T}{\partial r} \quad (101)$$

$$\left\{ \frac{\partial^2 \rho_r}{\partial r^2} + \frac{1}{r} \frac{\partial \rho_r}{\partial r} - \frac{\rho_r}{r^2} \right\} = \left\{ \frac{\beta - \alpha \gamma}{1 + \gamma} \right\} \frac{\partial \Delta T}{\partial r} \quad (102)$$

From Eq. (102),

$$\frac{\beta - \alpha \gamma}{1 + \gamma} = \frac{\frac{2\alpha + 2\mu\alpha}{1 - 2\mu} - \frac{\alpha}{1 - 2\mu}}{1 + \frac{1}{1 - 2\mu}} = \Gamma^{-1} \quad (103)$$

$$\Gamma = \frac{2}{\alpha} \left\{ \frac{1 - \mu}{1 + 2\mu} \right\} \quad (104)$$

Equation (102) may now be expressed as:

$$\Gamma \left\{ \frac{\partial^2 \rho_r}{\partial r^2} + \frac{1}{r} \frac{\partial \rho_r}{\partial r} - \frac{\rho_r}{r^2} \right\} = \frac{\partial \Delta T}{\partial r}, \quad (105)$$

$$\Gamma \left\{ \frac{\partial^2 \rho_r}{\partial r^2} + \frac{\partial}{\partial r} \left(\frac{\rho_r}{r} \right) \right\} = \frac{\partial \Delta T}{\partial r}, \quad (106)$$

and

$$r \frac{\partial}{\partial r} \left\{ \frac{\partial \rho_r}{\partial r} + \frac{\rho_r}{r} \right\} = \frac{\partial \Delta T}{\partial r} \quad (107)$$

Finally,

$$r \left\{ \frac{\partial \rho_r}{\partial r} + \frac{\rho_r}{r} \right\} + c = \Delta T(r) \quad (108)$$

Equation (108) is based on the following assumptions:

$$\begin{aligned} \Delta T &= \Delta T(r) \\ \rho_r &= \rho_r(r) \\ \rho_\theta &= 0 \\ \rho_z &= \alpha z \Delta T(r) \end{aligned}$$

I. General Thermostress Equations for Thin Plates in Rectangular Coordinates

The general thermostress equations in rectangular coordinates have the form

$$G \left\{ \nabla^2 + \frac{1}{1-2\mu} \vec{\nabla} \vec{\nabla} \cdot \right\} \vec{\rho} = \frac{E\alpha}{1-2\mu} \vec{\nabla} \Delta T \quad ; \quad (109)$$

or if

$$\beta = \frac{1}{1-2\mu} \quad ; \quad \gamma = \frac{1}{G} \frac{E\alpha}{1-2\mu} = \frac{\alpha 2(1+\mu)}{1-2\mu} \quad ,$$

then

$$(\nabla^2 + \gamma \vec{\nabla} \vec{\nabla} \cdot) \vec{\rho} = \beta \vec{\nabla} \Delta T \quad (110)$$

Expanding Eq. (110) yields

$$\left\{ \frac{\partial^2}{\partial x^2} + \frac{\partial^2}{\partial y^2} + \frac{\partial^2}{\partial z^2} \right\} (\rho_x \hat{i} + \rho_y \hat{j} + \rho_z \hat{k}) + \gamma \left\{ \frac{\partial}{\partial x} \hat{i} + \frac{\partial}{\partial y} \hat{j} + \frac{\partial}{\partial z} \hat{k} \right\} \left\{ \frac{\partial \rho_x}{\partial x} + \frac{\partial \rho_y}{\partial y} + \frac{\partial \rho_z}{\partial z} \right\} = \beta \left\{ \frac{\partial \Delta T}{\partial x} \hat{i} + \frac{\partial \Delta T}{\partial y} \hat{j} + \frac{\partial \Delta T}{\partial z} \hat{k} \right\} , \quad (111)$$

or

$$\begin{aligned} \frac{\partial^2 \rho_x}{\partial x^2} + \frac{\partial^2 \rho_x}{\partial y^2} + \frac{\partial^2 \rho_x}{\partial z^2} + \gamma \left\{ \frac{\partial^2 \rho_x}{\partial x^2} + \frac{\partial^2 \rho_y}{\partial x \partial y} + \frac{\partial^2 \rho_z}{\partial x \partial z} \right\} &= \beta \frac{\partial \Delta T}{\partial x} \\ \frac{\partial^2 \rho_y}{\partial x^2} + \frac{\partial^2 \rho_y}{\partial y^2} + \frac{\partial^2 \rho_y}{\partial z^2} + \gamma \left\{ \frac{\partial^2 \rho_x}{\partial y \partial x} + \frac{\partial^2 \rho_y}{\partial y^2} + \frac{\partial^2 \rho_z}{\partial y \partial z} \right\} &= \beta \frac{\partial \Delta T}{\partial y} \\ \frac{\partial^2 \rho_z}{\partial x^2} + \frac{\partial^2 \rho_z}{\partial y^2} + \frac{\partial^2 \rho_z}{\partial z^2} + \gamma \left\{ \frac{\partial^2 \rho_x}{\partial z \partial x} + \frac{\partial^2 \rho_y}{\partial z \partial y} + \frac{\partial^2 \rho_z}{\partial z^2} \right\} &= \beta \frac{\partial \Delta T}{\partial z} . \end{aligned} \quad (112)$$

Now, if for thin plates

$$\rho_z = \alpha z \Delta T(x, y) , \quad (113)$$

$$\text{then } \frac{\partial \rho_z}{\partial z} = \alpha \Delta T \quad (114)$$

$$\frac{\partial^2 \rho_z}{\partial x \partial z} = \alpha \frac{\partial \Delta T}{\partial x} \quad (115)$$

$$\frac{\partial^2 \rho_z}{\partial y \partial z} = \alpha \frac{\partial \Delta T}{\partial y} . \quad (116)$$

Assume ρ_x and ρ_y are not functions of z . Then

$$\frac{\partial^2 \rho_x}{\partial x^2} + \frac{\partial^2 \rho_x}{\partial y^2} + \gamma \left\{ \frac{\partial^2 \rho_x}{\partial x^2} + \frac{\partial^2 \rho_y}{\partial x \partial y} + \alpha \frac{\partial \Delta T}{\partial x} \right\} = \beta \frac{\partial \Delta T}{\partial x} \quad (117)$$

$$\frac{\partial^2 \rho_y}{\partial x^2} + \frac{\partial^2 \rho_y}{\partial y^2} + \gamma \left\{ \frac{\partial^2 \rho_x}{\partial x \partial y} + \frac{\partial^2 \rho_y}{\partial y^2} + \alpha \frac{\partial \Delta T}{\partial y} \right\} = \beta \frac{\partial \Delta T}{\partial y} \quad (118)$$

Simplifying terms,

$$(1 + \gamma) \frac{\partial^2 \rho_x}{\partial x^2} + \frac{\partial^2 \rho_x}{\partial y^2} + \gamma \frac{\partial^2 \rho_y}{\partial x \partial y} = (\beta - \gamma \alpha) \frac{\partial \Delta T}{\partial x} \quad (119)$$

$$(1 + \gamma) \frac{\partial^2 \rho_y}{\partial y^2} + \frac{\partial^2 \rho_y}{\partial x^2} + \gamma \frac{\partial^2 \rho_x}{\partial x \partial y} = (\beta - \gamma \alpha) \frac{\partial \Delta T}{\partial y} \quad (120)$$

J. Thermal Stress Deformation of a Thin Circular Plate With a Modified Correction for the z Component of Deformation

The problem associated with assuming that the ρ_z component of deformation obeys Eq. (113) is that the ρ_r contribution of deformation to the ρ_z component is not accounted for. The following derivation assumes that the material comprising the plate is largely incompressible and that changes in ρ_z may be directly related to changes in the ρ_r component. The coordinates for a circular plate are shown in Figure 9. For the thin circular plate, at r the deformation is ρ_r and at $r + \Delta r$ the deformation is

$$\rho(r + \Delta r) = \rho_r + \frac{\partial \rho_r}{\partial r} \bigg|_r \Delta r = \rho_r + \frac{\partial \rho_r}{\partial r} \Delta r \quad (121)$$

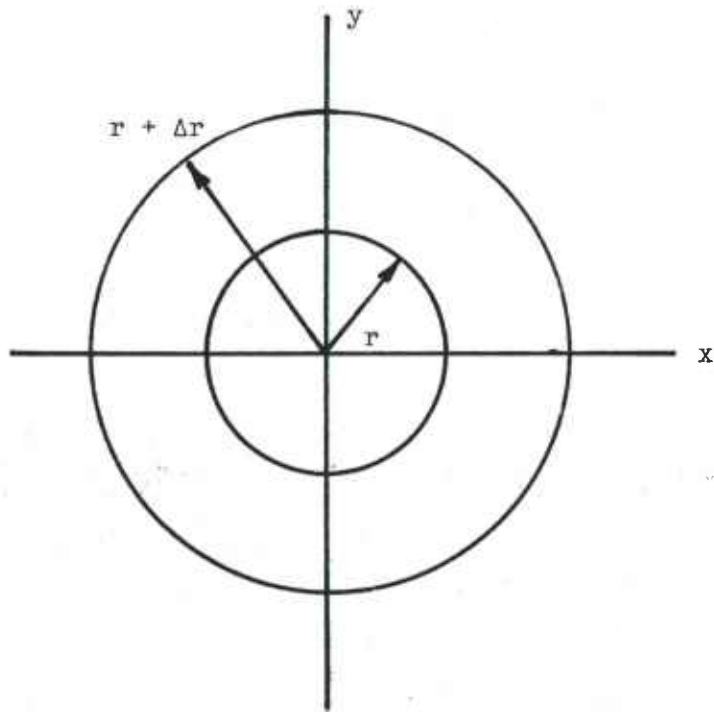


Figure 9. Coordinates for a circular plate.

The initial volume V_i of the material contained between r and $r + \Delta r$ is

$$V_i = \left[\Pi (r + \Delta r)^2 - \Pi r^2 \right] t, \quad (122)$$

where t is the plate thickness. Upon heating or cooling the plate, the new volume is

$$V_f = \left[\Pi \left\{ r + \Delta r + \rho_r + \frac{\partial \rho_r}{\partial r} \Delta r \right\}^2 - \Pi (r + \rho_r)^2 \right] t', \quad (123)$$

where t' is the new plate thickness.

Equating terms,

$$\left\{ \Pi (r + \rho_r' + \Delta r)^2 - \Pi (r + \rho_r)^2 \right\} t' = \left\{ \Pi (r + \Delta r)^2 - \Pi r^2 \right\} t$$

$$\rho_r' = \rho_r + \frac{\partial \rho_r}{\partial r} \Delta r$$

$$\begin{aligned} \left\{ r^2 + \rho_r'^2 + \Delta r^2 + 2r\rho_r' + 2r\Delta r + 2\rho_r'\Delta r - r^2 - \rho_r^2 - 2r\rho_r \right\} t' \\ = \left\{ r^2 + 2r\Delta r + \Delta r^2 - r^2 \right\} t \end{aligned} \quad (124)$$

Let

$$\rho_r' = \rho_r + \epsilon, \quad (125)$$

$$\text{where } \epsilon = \frac{\partial \rho_r}{\partial r} \Delta r.$$

Then

$$\rho_r'^2 = (\rho_r + \epsilon)^2 = \rho_r^2 + \epsilon^2 + 2\epsilon\rho_r \quad (126)$$

Substituting terms,

$$\begin{aligned} t' (\epsilon^2 + 2\epsilon\rho_r + \Delta r^2 + 2r\epsilon + 2r\Delta r + 2\rho_r\Delta r + 2\Delta r\epsilon) \\ = (2r\Delta r + \Delta r^2) t \end{aligned} \quad (127)$$

$$\frac{t'}{t} = \frac{2r\Delta r + \Delta r^2}{\left\{ \frac{\partial \rho_r}{\partial r} \Delta r \right\}^2 + 2 \left\{ \frac{\partial \rho_r}{\partial r} \Delta r \right\} \rho_r + \Delta r^2 + 2r \left\{ \frac{\partial \rho_r}{\partial r} \Delta r \right\} + 2r\Delta r + 2\rho_r\Delta r + 2\Delta r^2 \frac{\partial \rho_r}{\partial r}} \quad (128)$$

Simplifying and neglecting small terms,

$$\frac{t'}{t} = \frac{r}{\rho_r \frac{\partial \rho_r}{\partial r} + r \frac{\partial \rho_r}{\partial r} + r + \rho_r} \approx \frac{1}{1 + \frac{\partial \rho_r}{\partial r}} \quad (129)$$

Now,

$$\frac{t'}{2} = \frac{t}{2 \left(1 + \frac{\partial \rho_r}{\partial r} \right)} \quad (130)$$

And at $z = t/2$, the deformation is $t'/2 - t/2$.

Using the correction term of Eqs. (114) and (130),

$$\rho_z(r, z) = \alpha z \Delta T(r) + \frac{z}{1 + \left(\frac{\partial \rho_r}{\partial r} \right)} - z \quad (131)$$

$$\rho_z(r, z) = \alpha z \Delta T(r) + \frac{z - z - z \frac{\partial \rho_r}{\partial r}}{1 + \frac{\partial \rho_r}{\partial r}} \cong z \left(\alpha \Delta T(r) - \frac{\partial \rho_r}{\partial r} \right) \quad (132)$$

The thermostress equations in cylindrical coordinates are

$$(1 + \gamma) \left\{ \frac{\partial^2 \rho_r}{\partial r^2} + \frac{1}{r} \frac{\partial \rho_r}{\partial r} - \frac{\rho_r}{r^2} \right\} + \gamma \frac{\partial^2 \rho_z}{\partial r \partial z} = \beta \frac{\partial \Delta T}{\partial r}$$

$$(1 + \gamma) \left\{ \frac{\partial^2 \rho_r}{\partial r^2} + \frac{\partial}{\partial r} \left(\frac{\rho_r}{r} \right) \right\} + \gamma \frac{\partial^2 \rho_z}{\partial r \partial z} = \beta \frac{\partial \Delta T}{\partial r} \quad (133)$$

Substituting Eq. (132) into Eq. (133),

$$(1 + \gamma) \left\{ \frac{\partial^2 \rho_r}{\partial r^2} + \frac{\partial}{\partial r} \left(\frac{\rho_r}{r} \right) \right\} + \gamma \frac{\partial}{\partial r} \left\{ \alpha \Delta T - \frac{\partial \rho_r}{\partial r} \right\} = \beta \frac{\partial \Delta T}{\partial r}$$

$$(1 + \gamma) \left\{ \frac{\partial^2 \rho_r}{\partial r^2} \right\} + \left\{ \frac{\partial}{\partial r} \left(\frac{\rho_r}{r} \right) \right\} (1 + \gamma) - \gamma \frac{\partial^2 \rho_r}{\partial r^2} + \gamma \alpha \frac{\partial \Delta T}{\partial r} = \beta \frac{\partial \Delta T}{\partial r}$$

$$\frac{\partial^2 \rho_r}{\partial r^2} + (1 + \gamma) \frac{\partial}{\partial r} \left\{ \frac{\rho_r}{r} \right\} = (\beta - \alpha \gamma) \frac{\partial \Delta T}{\partial r}$$

$$(\beta - \alpha \gamma) \frac{\partial \Delta T}{\partial r} = \frac{\partial}{\partial r} \left\{ \frac{\partial \rho_r}{\partial r} + (1 + \gamma) \frac{\rho_r}{r} \right\} \quad (134)$$

Integrating,

$$\Delta T = \frac{1}{\beta - \alpha\gamma} \left\{ \frac{\partial \rho_r}{\partial r} + (1 + \gamma) \frac{\rho_r}{r} \right\} + C \quad (135)$$

Suppose the plate is infinite in extent; i.e., @ $r = \infty$, $\rho_r = 0$, $\partial \rho_r / \partial r = 0$, and $\Delta T = 0$. This implies that $C = 0$. Therefore,

$$\Delta T = \frac{1}{\beta - \alpha\gamma} \left\{ \frac{\partial \rho_r}{\partial r} + (1 + \gamma) \frac{\rho_r}{r} \right\} \quad (136)$$

for an infinite plate.

K. Least Squares Method of Differentiating Experimental Data

Assume that N measurements of radial deformation (ρ_i) were taken in some region of a thin circular plate. Assume that the deformation in this region is given by

$$\rho_r = Ar^3 + Br^2 + Cr + D \quad (137)$$

Forming the square of the difference (difference function) between the curve given by Eq. (137) and the experimental data [5],

$$\delta_i = \sum_{i=1}^N \left[\rho_i - (Ar_i^3 + Br_i^2 + Cr_i + D) \right]^2 \quad (138)$$

Differentiating with respect to the unknowns to obtain an extrema,

$$\frac{\partial \delta_i}{\partial A} = 0 = \sum_{i=1}^N \left[\rho_i - A r_i^3 - B r_i^2 - C r_i - D \right] r_i^3$$

$$\frac{\partial \delta_i}{\partial B} = 0 = \sum_{i=1}^N \left[\rho_i - A r_i^3 - B r_i^2 - C r_i - D \right] r_i^2$$

$$\frac{\partial \delta_i}{\partial C} = 0 = \sum_{i=1}^N \left[\rho_i - A r_i^3 - B r_i^2 - C r_i - D \right] r_i$$

$$\frac{\partial \delta_i}{\partial D} = 0 = \sum_{i=1}^N \left[\rho_i - A r_i^3 - B r_i^2 - C r_i - D \right] \quad . \quad (139)$$

Let $\Sigma = \sum_{i=1}^N$

and rearrange terms to obtain

$$A \Sigma r_i^6 + B \Sigma r_i^5 + C \Sigma r_i^4 + D \Sigma r_i^3 = \Sigma \rho_i r_i^3$$

$$A \Sigma r_i^5 + B \Sigma r_i^4 + C \Sigma r_i^3 + D \Sigma r_i^2 = \Sigma \rho_i r_i^2$$

$$A \Sigma r_i^4 + B \Sigma r_i^3 + C \Sigma r_i^2 + D \Sigma r_i = \Sigma \rho_i r_i$$

$$A \Sigma r_i^3 + B \Sigma r_i^2 + C \Sigma r_i + D N = \Sigma \rho_i \quad . \quad (140)$$

$$\begin{aligned}
\text{Let } R6 &= \sum r_i^6 & S3 &= \sum \rho_i r_i^3 \\
R5 &= \sum r_i^5 & S2 &= \sum \rho_i r_i^2 \\
R4 &= \sum r_i^4 & S1 &= \sum \rho_i r_i \\
R3 &= \sum r_i^3 & S0 &= \sum \rho_i \\
R2 &= \sum r_i^2 \\
R1 &= \sum r_i \\
R0 &= N
\end{aligned} \tag{141}$$

$$\text{Then } S3 = A \cdot R6 + B \cdot R5 + C \cdot R4 + D \cdot R3$$

$$S2 = A \cdot R5 + B \cdot R4 + C \cdot R3 + D \cdot R2$$

$$S1 = A \cdot R4 + B \cdot R3 + C \cdot R2 + D \cdot R1$$

$$S0 = A \cdot R3 + B \cdot R2 + C \cdot R1 + D \cdot R0 \quad . \tag{142}$$

Equation (142) may be expressed in matrix form as

$$\begin{bmatrix} R6 & R5 & R4 & R3 \\ R5 & R4 & R3 & R2 \\ R4 & R3 & R2 & R1 \\ R3 & R2 & R1 & R0 \end{bmatrix} \cdot \begin{bmatrix} A \\ B \\ C \\ D \end{bmatrix} = \begin{bmatrix} S3 \\ S2 \\ S1 \\ S0 \end{bmatrix} \tag{143}$$

Equation (143) may be solved for A, B, C, and D--thus giving the equation for ρ_r with a least squares curve fit. These curves can then be more readily differentiated in the thermostress equations to obtain better results.

L. Polynomial Approximation to the Thin Plate Thermostress Equation in Cylindrical Coordinates

The thin plate thermostress equation in cylindrical coordinates may be given as

$$\Gamma \left\{ \frac{\partial \rho_r}{\partial r} + \frac{\rho_r}{r} \right\} + C = \Delta T(r)$$

$$\Gamma = \frac{2}{\alpha} \left\{ \frac{1 - \mu}{1 + 2\mu} \right\} \quad (144)$$

The difference in temperature T_{r-R_0} between location r and R_0 is given as

$$\Delta T_{r-R_0} = -\Gamma \left\{ \frac{\partial \rho_r}{\partial r} + \frac{\rho_r}{r} \right\} \bigg|_r^{R_0} \quad (145)$$

Suppose

$$\rho_r = Ar^2 + Br + C \quad (146)$$

for a thin plate. Then

$$\frac{\partial \rho_r}{\partial r} = 2Ar + B, \quad (147)$$

and

$$\begin{aligned}
\Delta T_{r-R_0} &= -\Gamma \left\{ 2Ar + B + Ar + B + \frac{C}{r} \right\} \Big|_r^{R_0} \\
\Delta T_{r-R_0} &= -\Gamma \left\{ 3Ar + 2B + \frac{C}{r} \right\} \Big|_r^{R_0} \\
\Delta T_{r-R_0} &= -\Gamma \left\{ 3AR_0 + 2B + \frac{C}{R_0} - 3Ar - 2B - \frac{C}{r} \right\} \quad . \quad (148)
\end{aligned}$$

But $C = 0$, since $\rho_r = 0$ at $r = 0$. Therefore

$$\begin{aligned}
\Delta T_{r-R_0} &= -3A\Gamma [R_0 - r] \\
\Delta T_{r-R_0} &= 3A\Gamma [r - R_0] \quad . \quad (149)
\end{aligned}$$

Now,

$$\frac{\partial \Delta T}{\partial r} = \Gamma \frac{\partial}{\partial r} \left\{ \frac{\partial \rho_r}{\partial r} + \frac{\rho_r}{r} \right\} \quad . \quad (150)$$

Suppose

$$\rho_r = Ar^2 + Br \quad , \quad (151)$$

then

$$\Gamma \frac{\partial}{\partial r} \{ 2Ar + B + Ar + B \} = \frac{\partial \Delta T}{\partial r} \quad (152)$$

or

$$\frac{\partial \Delta T}{\partial r} = 3\Delta T \quad . \quad (153)$$

Equation (153) may be used to estimate thermal gradients from experimental data.

III. EXPERIMENTAL EXAMPLES

The following three cases were used to test the theory presented in Section II. Two problems are treated in this section:

- a. The heating of a thin circular flat plate at its center by external heat generation.
- b. The uniform heating of a rod.

The thin circular flat plate problem is treated in Sections IIIB and IIID, and the uniform heating of a rod is treated in Section IIIC.

A. Computer System for Analyzing Laser Speckle Interferograms

Figure 10 illustrates the automated system used to analyze laser speckle interferograms. A description of the system and its functional components are documented in reference [3]. The system was used in the manual mode, and the computer programs used to control the system are listed in the appendix.

B. Temperature Change Measurements for a Heated Circular Flat Plate (Case I)

This test was conducted to examine the accuracy in measuring a temperature change ΔT in a circular flat plate using laser speckle interferometry. The plate may be classed as a thin circular flat plate subject to a heat source located at the center. The heat source was obtained from electrical resistive heating located at the center of the plate. The resulting temperature profile of the plate tends to be a function of the radial distance from the center of the plate.

Figure 11 illustrates the basic laboratory configuration for measuring temperature changes in circular flat plates subject to a radial symmetric temperature distribution. In the test, an 18.0-inch diameter, 0.125-inch-thick aluminum plate (Figure 12) was mounted onto a heater element support (Figure 13). The heater element support was also aluminum and was covered with a 0.25-inch-thick layer of

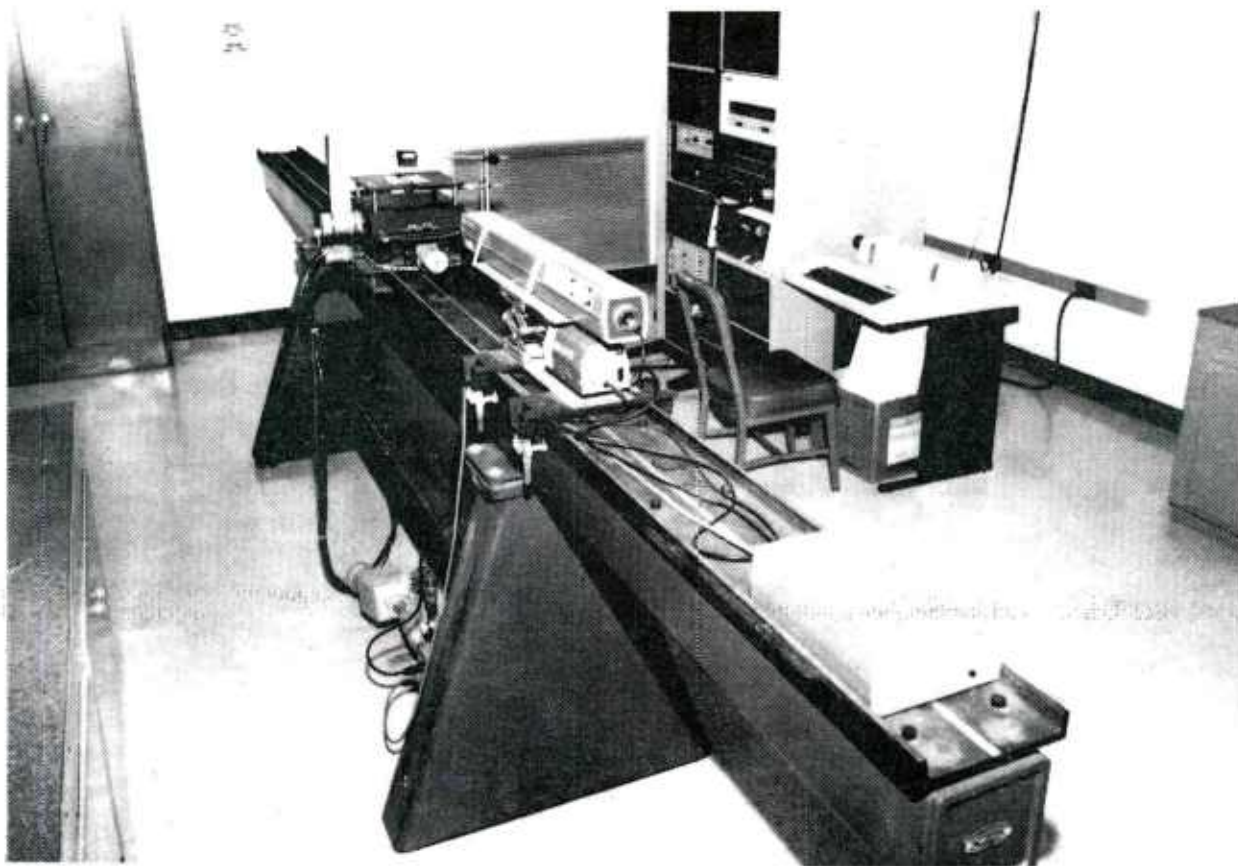


Figure 10. System used to analyze laser speckle interferograms.

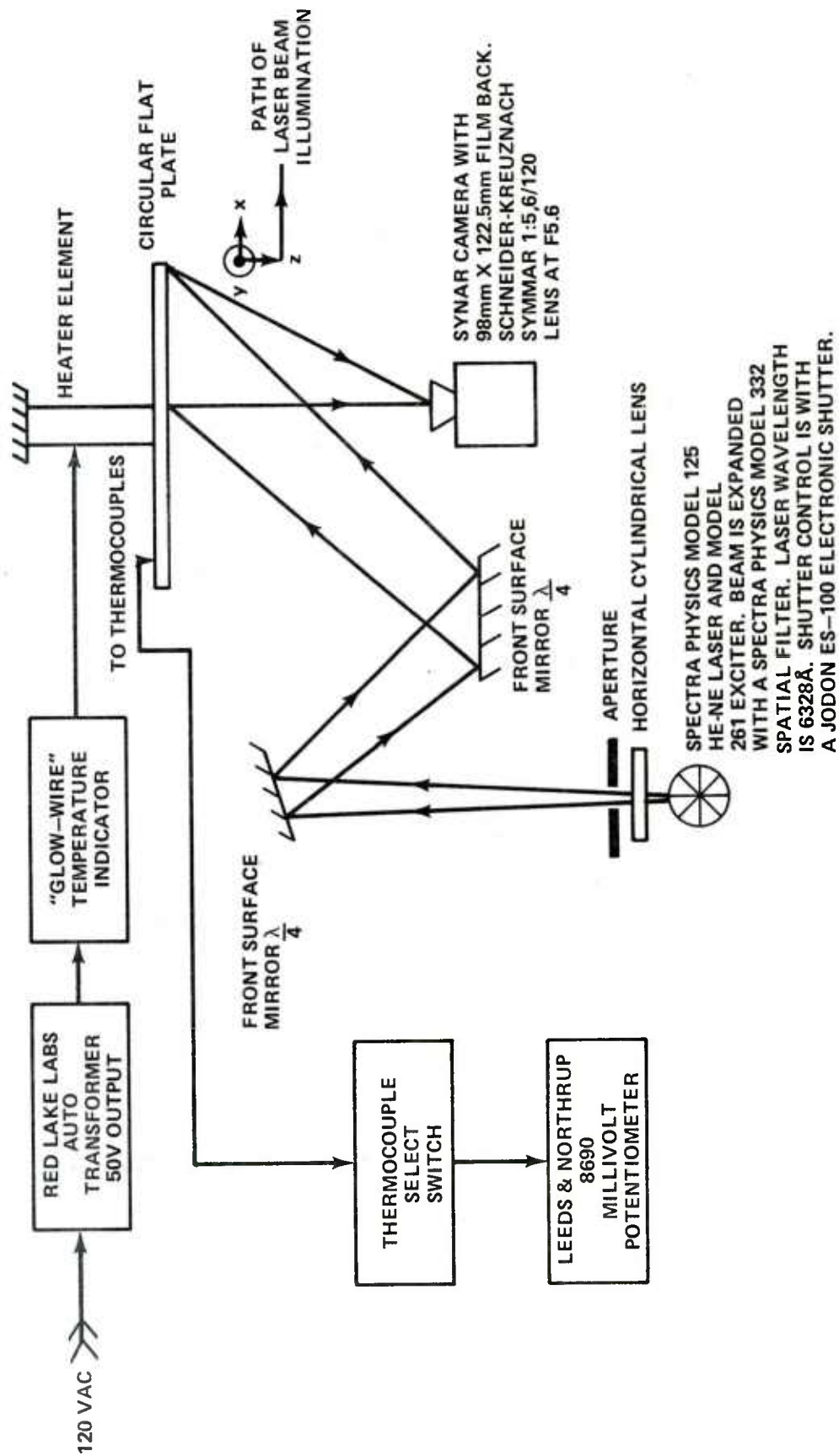
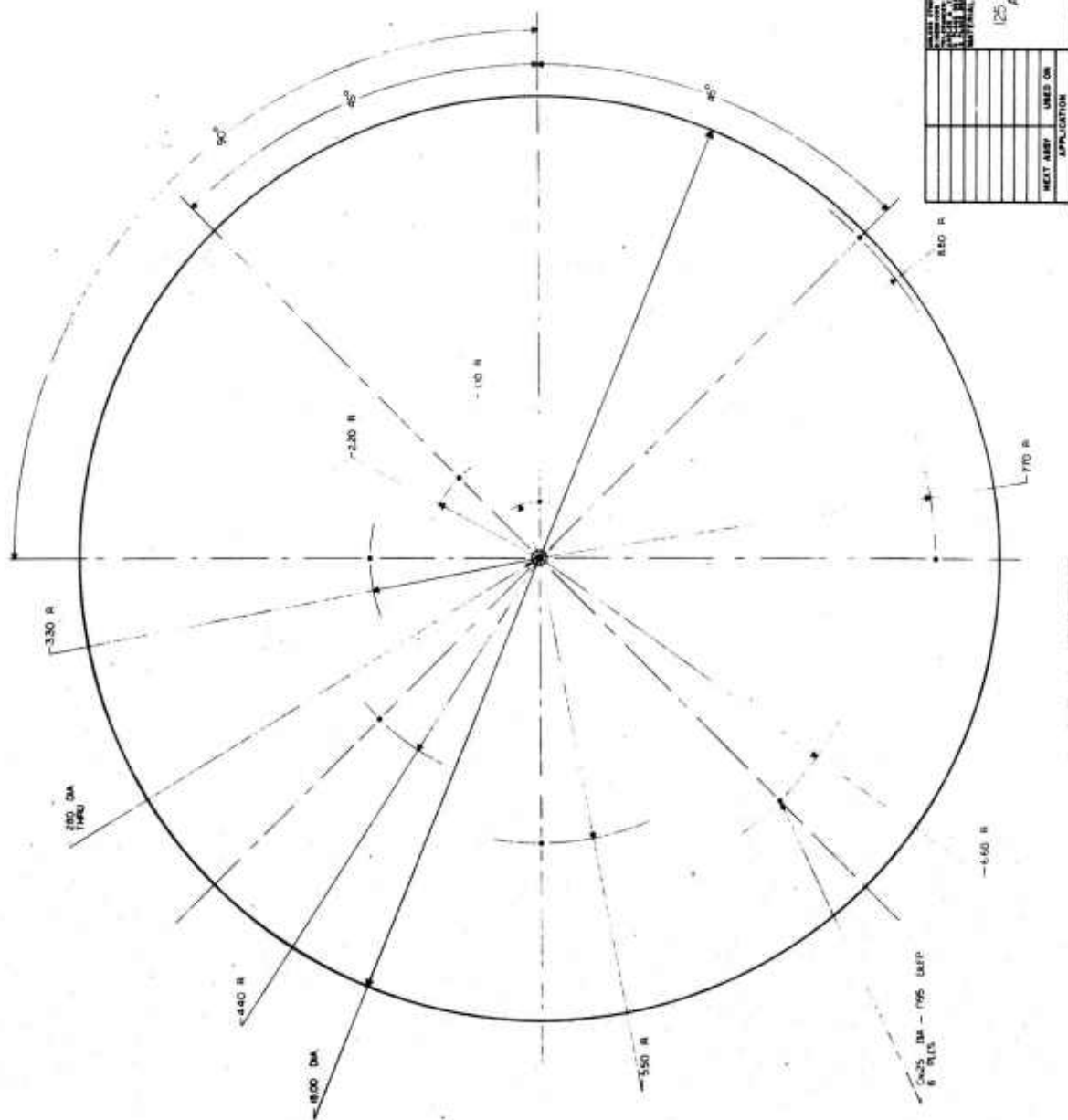


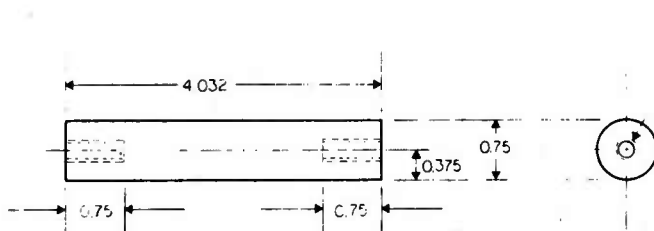
Figure 11. Basic laboratory configuration for examining the deformation of circular heated flat plates.



NOTES:
1. HONEY, BARS, BREAK SHARP EDGES.
2. 1/2 IN. THK

U.S. ARMY MISSILE COMMAND REDSTONE ARSENAL, ALABAMA		DATE: JAN. 1960 DESIGNED BY: [blank] CHECKED BY: [blank] ENGINEER: [blank]		U.S. ARMY MISSILE COMMAND REDSTONE ARSENAL, ALABAMA	
THERMOSTRESS - 1		125 IN. THK ALUM.		THERMOSTRESS - 1	
APPROVED BY: [blank]		APPROVED BY: [blank]		APPROVED BY: [blank]	
D18876		SK-NOT-038		D18876	
SCALE 1/1		SHEET 1 OF 1		SHEET 1 OF 1	

Figure 12. Circular flat plate.



DRILL AND TAP FOR
 $\frac{1}{4}$ -20-UNC-2B
 2 PLCS

NOTES:

1. REMOVE BURRS, BREAK SHARP EDGES.

3/3/79
Shurt

		UNLESS OTHERWISE SPECIFIED DIMENSIONS ARE IN INCHES TOLERANCES: FRACTIONS ± ANGLES ± 3 PLACE DECIMALS ± 2 PLACE DECIMALS ±		U.S. ARMY MISSILE COMMAND REDSTONE ARSENAL, ALABAMA	
		MATERIAL		THERMOSTRESS - 1	
		ALUM		DATE 7 DEC. 1979	
				PREPARED A. DEMSEY	
				CHECKED J. H. H.	
				ENGINEER	
				APPROVED BY ORDER OF CG. USAMICOM	
				APPROVED	
NEXT ASSY		USED ON		SIZE CODE IDENT NO. DRAWING NO.	
				C 18876 SK-NDT-036	
APPLICATION				SCALE 1/1 SHEET 1 OF 3	

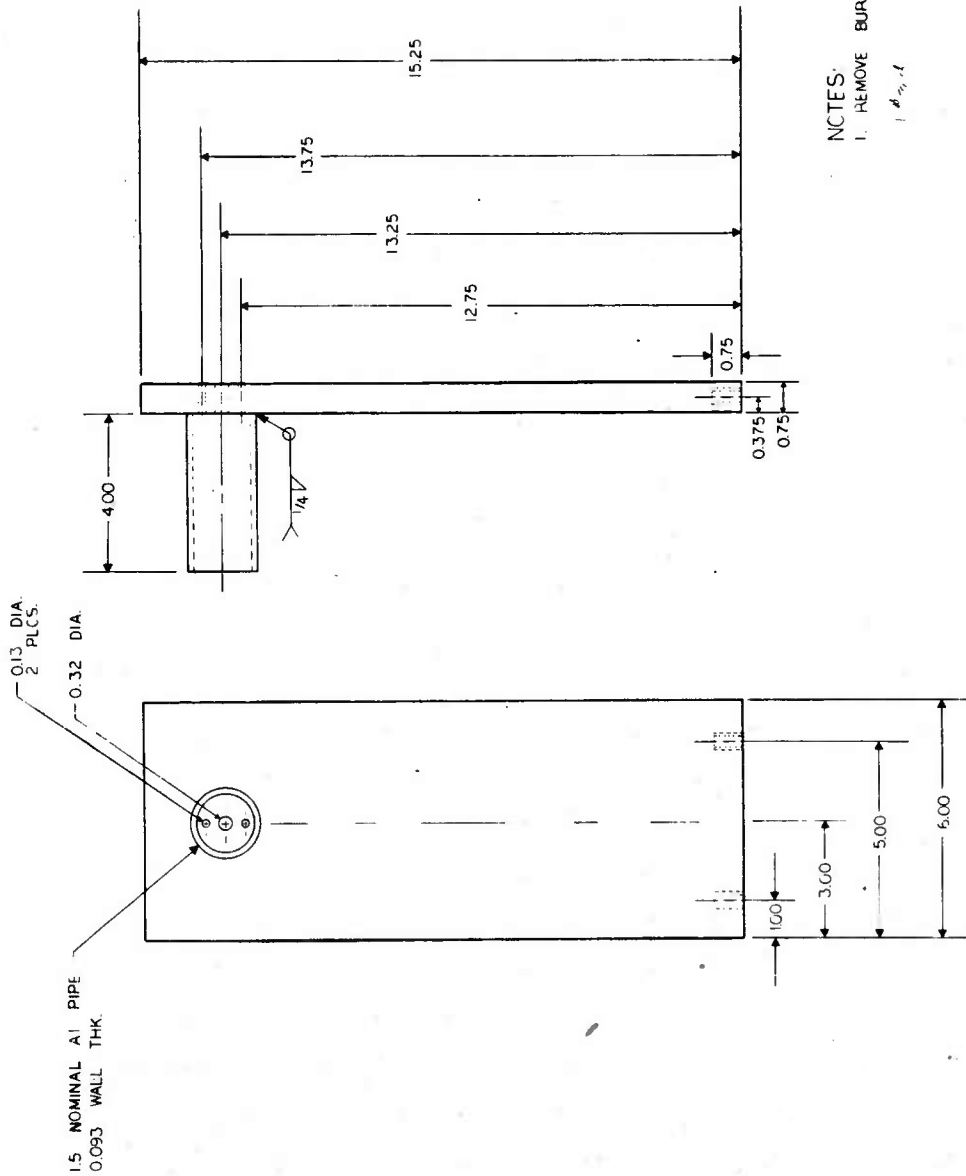
Figure 13. Heater element support.

compressed K-wool. Nichrome wire was wrapped around the circumference and length of the support to serve as a heater element. Again, K-wool was wrapped around the wire to electrically insulate it from any metal. The plate and heater were then inserted into the plate heater unit holder (Figure 14). In order to provide electric power access, 0.13-inch-diameter holes were provided in the holder. The plate heater holder was then bolted to the heater unit support base (Figure 15), which was then bolted to an NRC air table for laser speckle work.

In order to determine the accuracy in measuring temperature fields with laser speckle, a series of .0625-inch-diameter, .095-inch-deep holes were drilled at various radial distances on the circular plate (Figure 12). Copper-constantan thermocouples were attached in each of these holes using a conductive epoxy. This compound is available from Ablestik Laboratories, 833 West 182d Street, Gardena, CA 90248, and consisted of the following:

- . Ablebond 163-4, part C pure copper powder
(4 parts)
- . Ablebond 163-4, part A resin component
(2 parts)
- . Ablebond 163-4, part B hardener component
(1 part)

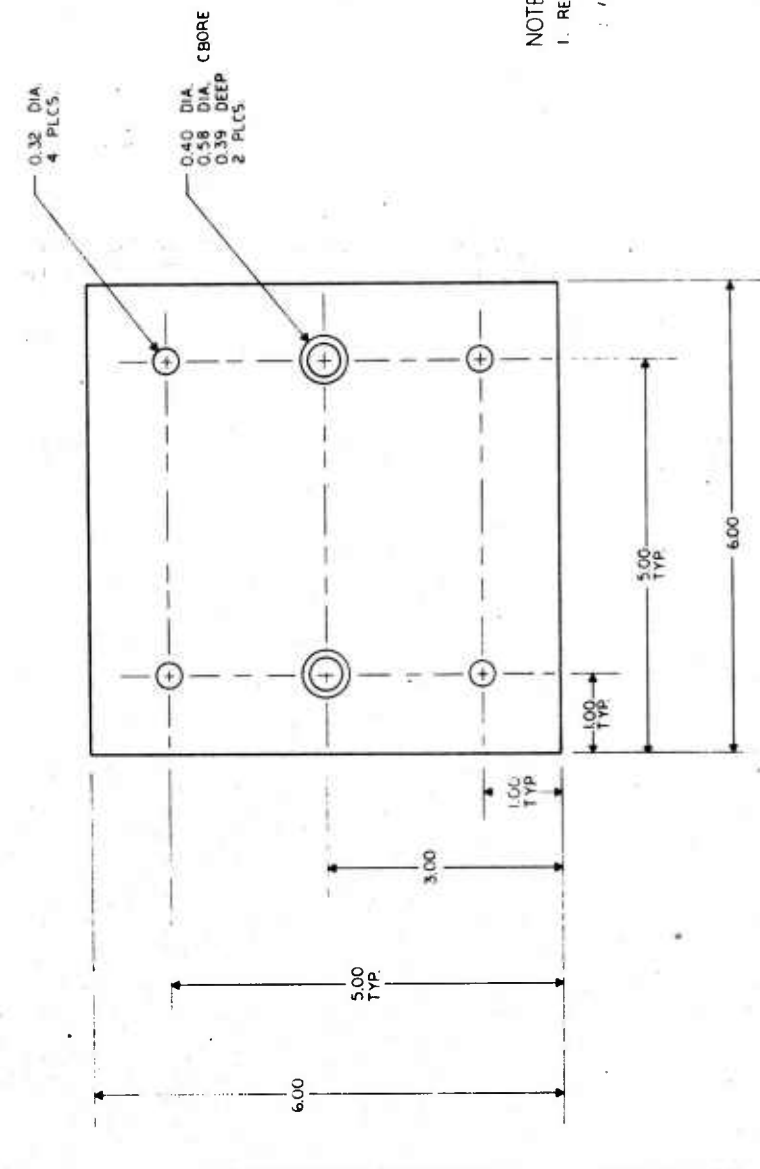
Figure 16 illustrates a typical thermocouple attached to the aluminum plate. It is unfortunate that a significant amount of heat can be conducted away from the thermocouple attachment point with this design, but it was the best known alternative available. A better alternative would have been to use a semiconductor thermal radiation detector or liquid crystals, but these were not readily available. Figure 17 illustrates the complete assembly of eight thermocouples which were mounted on the circular flat plate. Each of the thermocouples, including a reference at 0° C, was individually switched to a Leeds and Northrup 8690 potentiometer, using the electrical schematic shown in Figure 18. The rotary switch is shown in Figure 19. A voltage divider, using 1-k Ω resistors, was used to plot thermocouple output versus thermocouple number. The reference thermocouple temperature at 0° C



NOTES:
1. REMOVE BURRS BREAK SHARP EDGES.

UNLESS OTHERWISE SPECIFIED DIMENSIONS ARE IN INCHES FRACTIONS 2 DECIMALS 3 PLACES DECIMALS 3005		U.S. ARMY MISSILE COMMAND REDSTONE ARSENAL, ALABAMA	
DATE 14 DEC. 1979		THERMOSHEAT - 1	
PREPARED A. DEMPSEY		SIZE CODE IDENT NO. DRAWING NO.	
CHECKED JKL		C18876 SK-NDT-036	
ENGINEER		SCALE 1/2	
APPROVED BY ORDER OF CG.		SHEET 3 OF 3	
UNANIMOUS			
APPROVED			
MATERIAL			
ALUM.			
NEXT ASSY		USED ON	
APPLICATION			

Figure 14. Plate heater unit holder.



NOTES:
1. REMOVE BURRS, BREAK SHARP EDGES.

U.S. ARMY MISSILE COMMAND REDSTONE ARSENAL, ALABAMA		THERMOSTRESS - 1	
DATE 13 DEC. 1979 PREPARED A DEMFSEY CHECKED JMS ENGINEER APPROVED BY ORDER OF CO. JANCON		SIZE CODE IDENT NO. DRAWING NO. C18876 SK-NDT-036	
MATERIAL 0.75 IN THK ALUM		SCALE 1/1	
APPLICATION NEXT ASSY USED ON		SHEET 2 OF 3	

Figure 15. Heater unit support base.

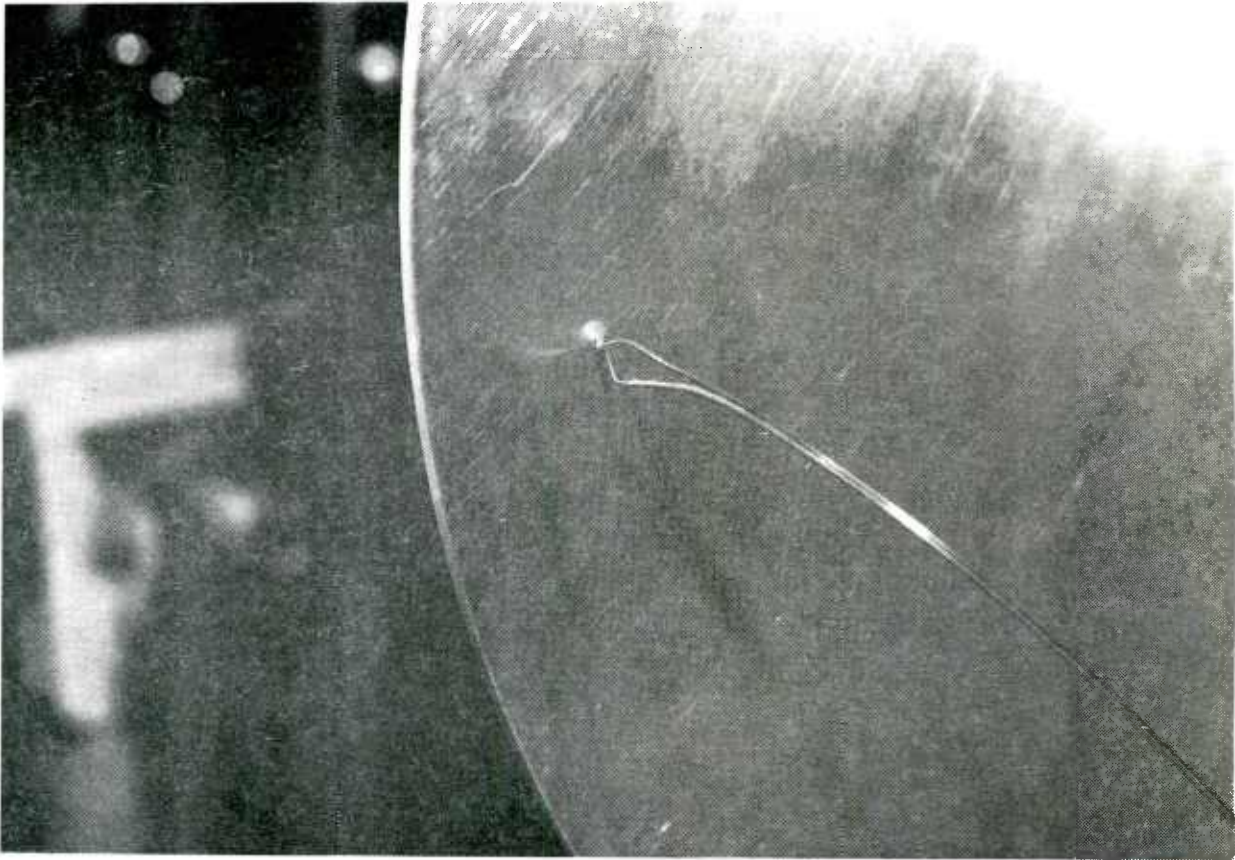


Figure 16. Attachment of iron-constantan thermocouples to aluminum plate.

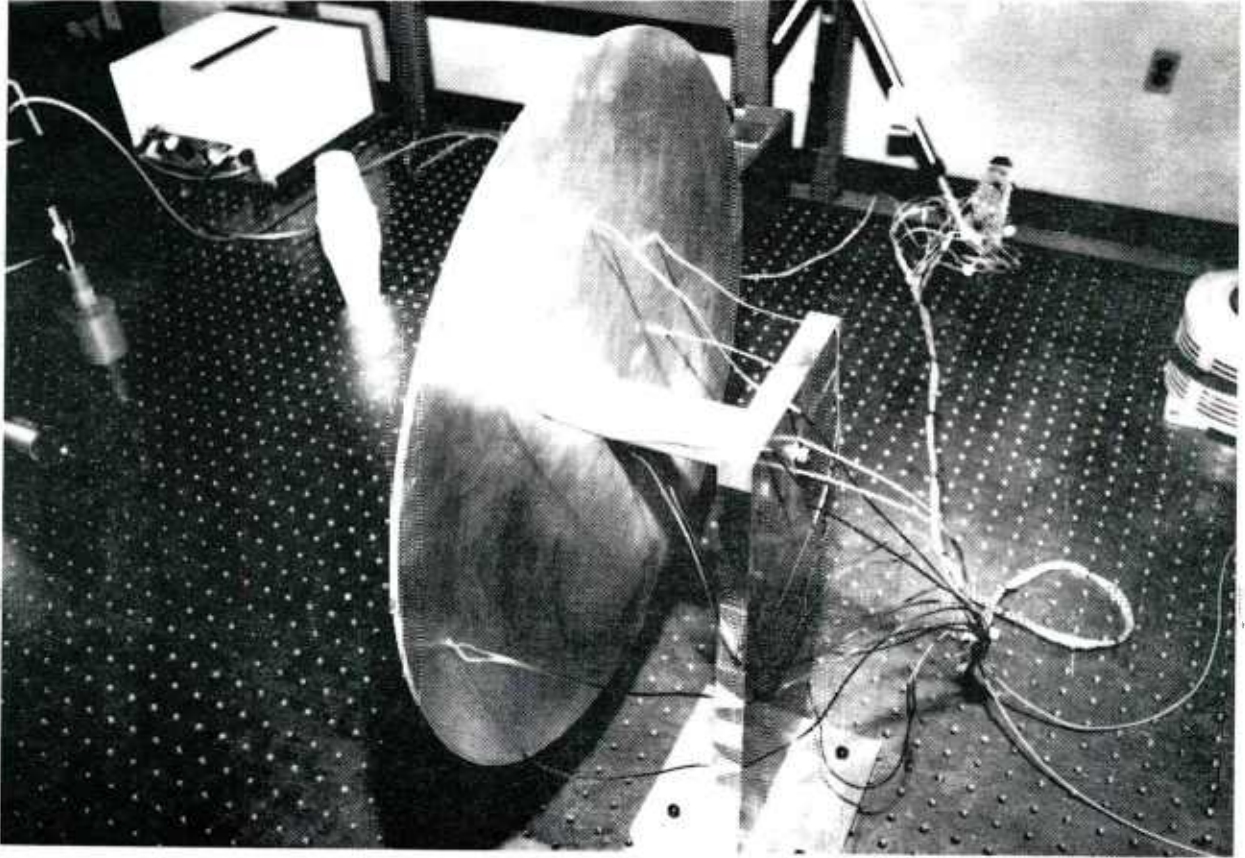


Figure 17. Complete assembly of thermocouples on the circular flat plate.

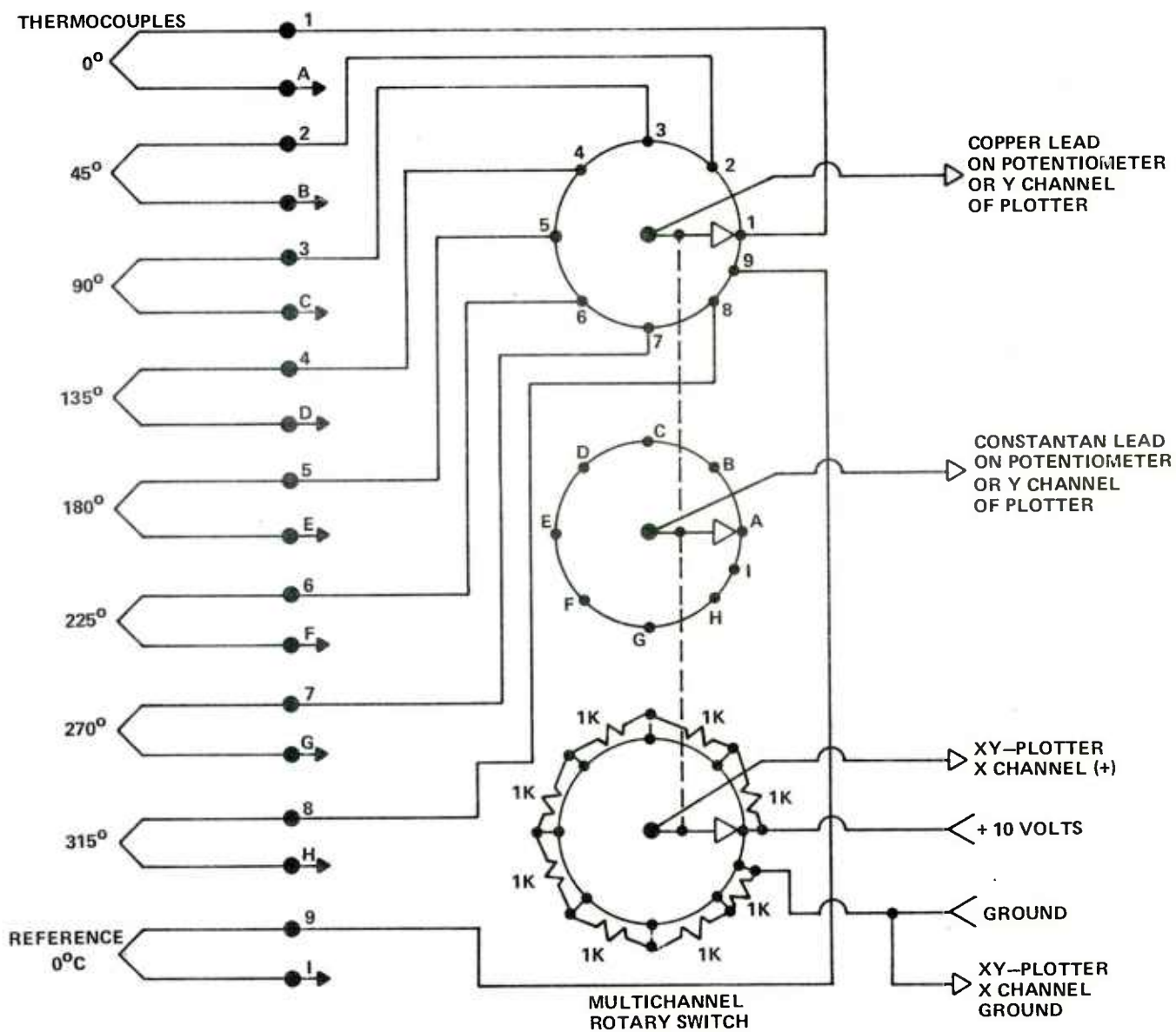


Figure 18. Thermocouple switch network schematic.

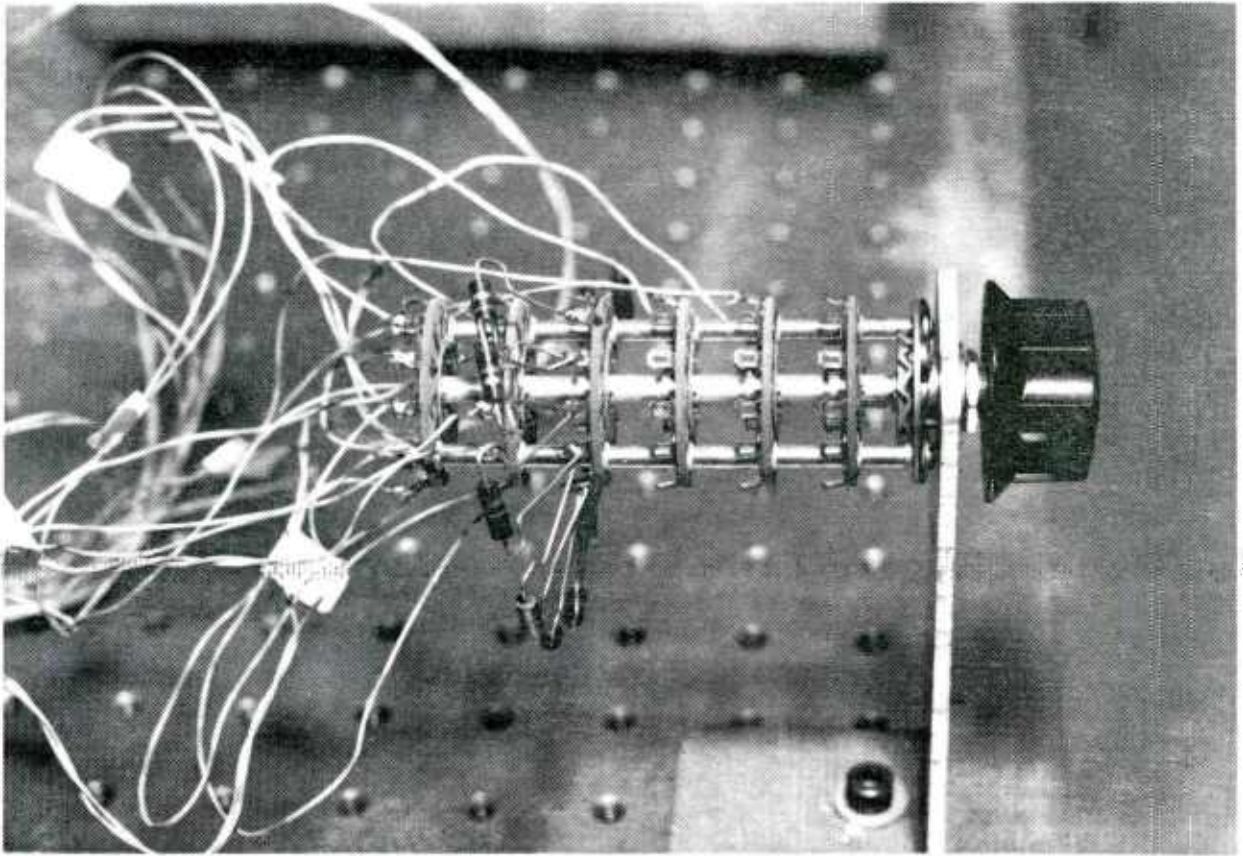


Figure 19. Thermocouple rotary switch.

was obtained from a reference bath (Figure 20). This device could provide a cold junction for several hours before any ice replacement was needed. Figure 21 is a photograph of the Leeds and Northrup Millivolt Potentiometer.

In order to supply electrical power to the circular flat plate heater element (Figure 11), a Redlake Labs Autotransformer at about 50-V-a.c. output (variable) was used. A piece of Nichrome wire was placed in series with the heater element to observe the plate heater performance. When the "glow wire" was a bright red, the proper current flow was presented in the heater assembly. At this point, the maximum rise in plate temperature with time was observed.

Laser illumination of the plate was accomplished by expanding the output of a 6328 Å spectra physics Model 125, 50-mW He-Ne laser. A spectra physics Model 332 spatial filter was used for this purpose. Exposure control of the laser was performed using a Jodon ES-100 electronic shutter (Figure 22). The output of the laser was passed through a horizontally oriented cylindrical lens to produce a narrow concentrated rectangular beam of light, which measured 10.2 mm by 228.6 mm in the horizontal 0-direction on the circular plate. Beam control was performed using two $\lambda/4$ front surface mirrors and an aperture for beam expansion.

In the test, an attempt to measure the temperature rise at station #1 ($r = 1.1$ in.) was made. Two 32-second exposures were made using AGFA GAVAERT holographic film. The initial station #1 temperature was 81° F when the first exposure was made. The plate was then heated to a thermocouple measured temperature of 112° F, and a second laser exposure was made. The net temperature change at station #1 was 31° F, as measured with the thermocouple.

Test Results - Case I:

$$S = \frac{9.0}{3.88} = 2.3195 \text{ for a 9-inch-radius plate}$$

$$f = 74 \text{ in.}$$

$$\left. \begin{array}{l} T_i \approx 81^\circ \text{ F} \\ T_f \approx 112^\circ \text{ F} \end{array} \right\} \text{ measured with thermocouple}$$

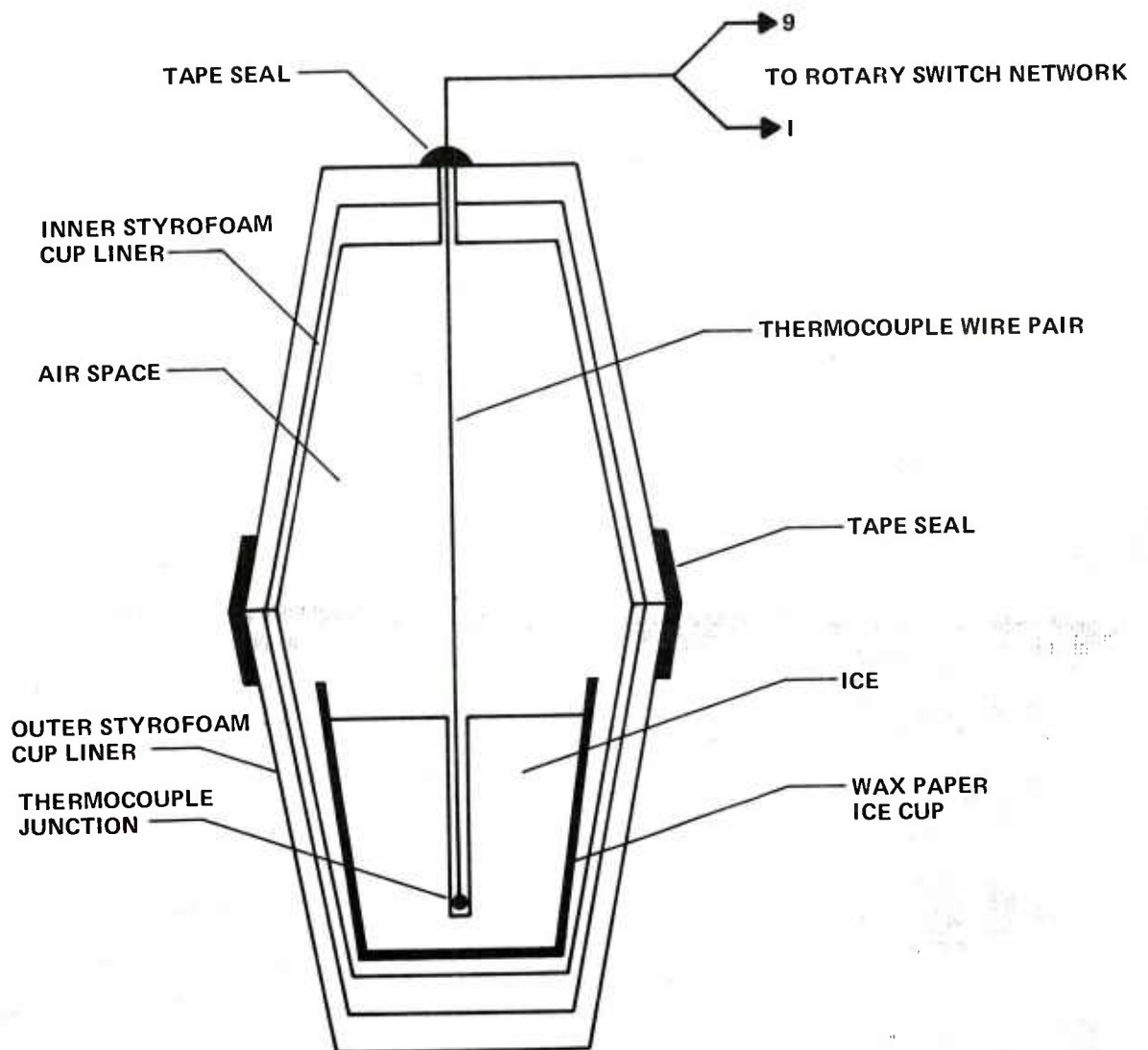


Figure 20. Reference junction ice bath.

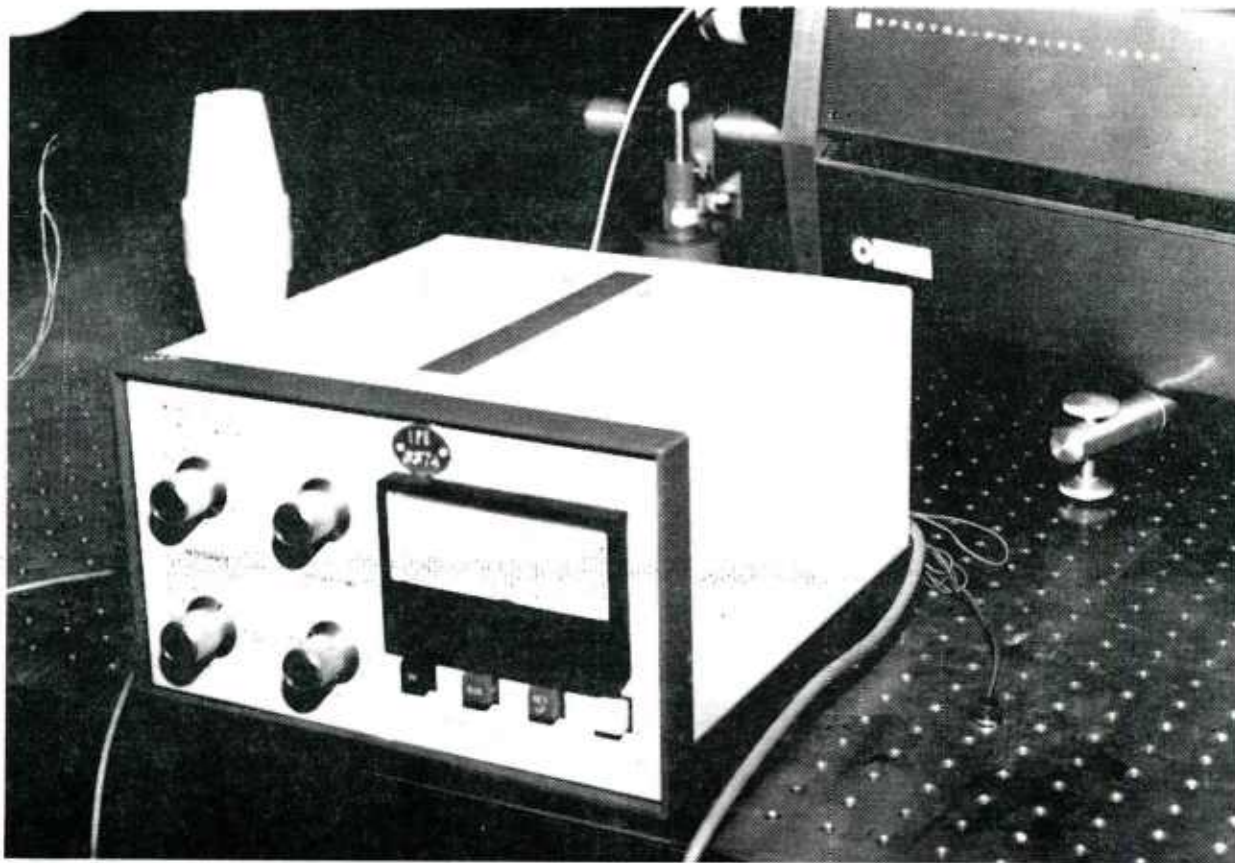


Figure 22. Jodon ES-100 electronic shutter system.

Table 1 illustrates the data obtained from the interferogram. For this data, r' is the radial distance on the interferogram and r is the radial distance on the plate. $\chi'(r)$ is the measured fringe spacing. The sign associated with $\chi'(r)$ determines the direction of plate translation upon heating; (+) refers to motion in the positive X direction. Table 2 shows the data of Table 1 corrected for true relative translation, with the center of the plate having zero translation.

Figure 23 illustrates the variation of $\gamma(r)$ with r . In order to differentiate $\gamma(r)$ with respect to r , a quadratic curve fit of Figure 23 is utilized.

$$\gamma(r) = \frac{r}{\chi(r)} \cong Ar + Br^2 + C \quad (154)$$

The data for Eq. (72) may be tabulated as

r	$\gamma(r)$
.30	0
1.23	.07662
2.44	.19012

Solving the simultaneous linear equations in A, B, and C results in

$$\begin{aligned} A &= .07415 \\ B &= .0054 \\ C &= -.02273 \end{aligned} ,$$

and

$$\gamma(r) = .07415r + .0054r^2 - .02273$$

TABLE 1. CASE I INTERFEROMETRIC DATA

r'	r	$\chi'(r)$	$1/\chi'(r)$
.13	.30	-2.86	-.34965
1.05	2.44	-3.68	-.27173
.53	1.23	-3.48	-.28735
1.63	3.78	-4.68	-.21367
2.19	5.08	-7.02	-.14245
3.44	7.98	+5.75	+.17391
3.88	9.00	+3.93	+.25445

TABLE 2. CORRECTED CASE I INTERFEROMETRIC DATA

r	$1/\chi(r)$	$\gamma(r)$
.30	0	0
2.44	.07792	.19012
1.23	.06230	.07662
3.78	.13598	.51400
5.08	.20720	1.05257
7.98	.52356	4.17800
9.00	.60410	5.43690

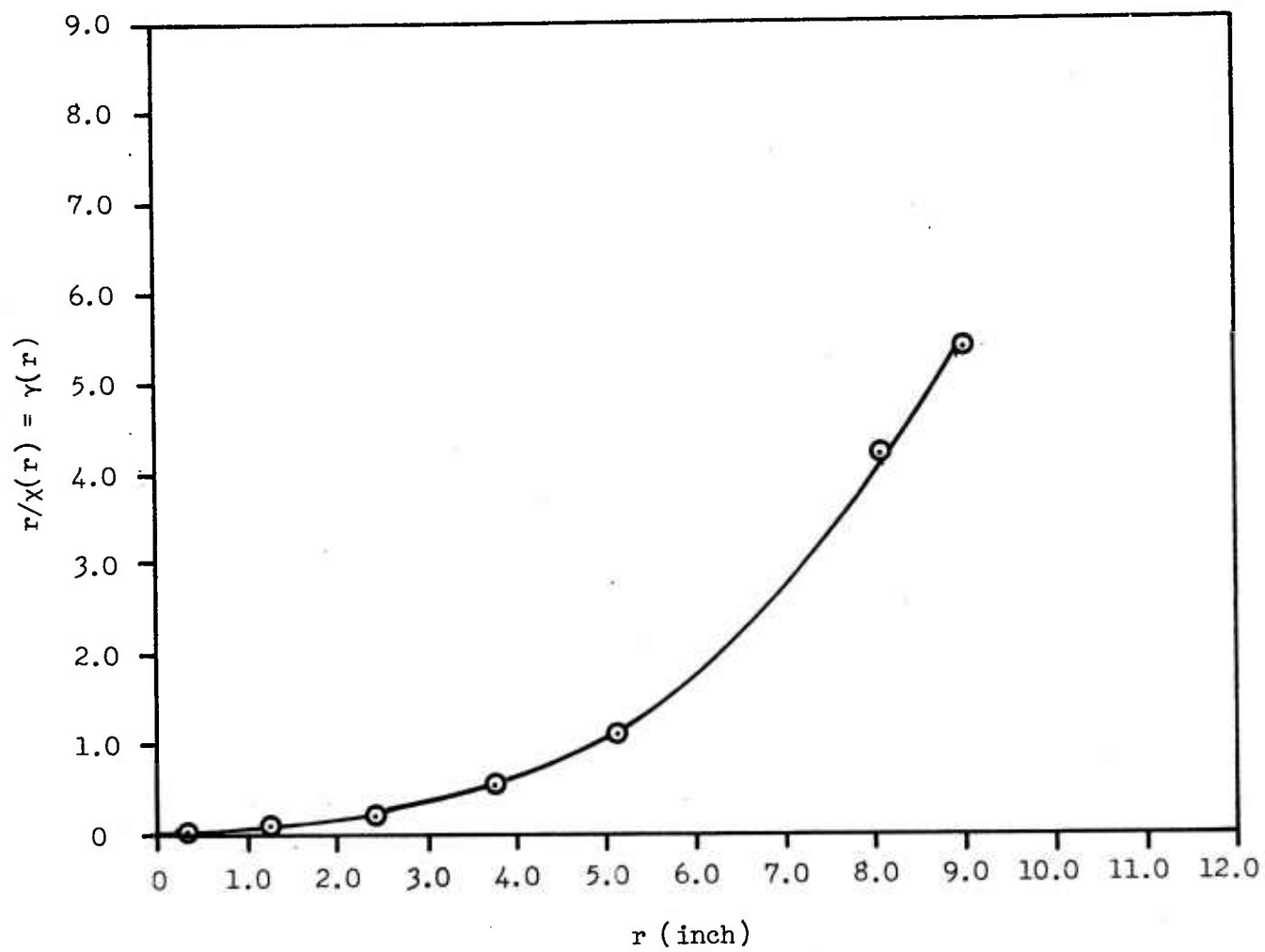


Figure 23. Case I $\gamma(r)$ versus r .

Now from Eq. (55),

$$\beta = \frac{\lambda f S}{2\alpha} \left(\frac{1 - \mu}{\mu} \right) ,$$

where

$$\begin{aligned} \lambda &= 6328\text{\AA} = 2.4913 \times 10^{-5} \text{ in.} \\ f &= 74.0 \text{ in.} \\ S &= 2.3195 \\ \alpha (\text{Aluminum}) &= 24 \times 10^{-6} / ^\circ\text{C} \\ \mu (\text{Aluminum}) &= .3 \end{aligned}$$

Now,

$$\partial \frac{\gamma(r)}{\partial r} = .07415 + .0108r$$

$$\beta = 207.86$$

$$\frac{1}{r} \partial \frac{\gamma(r)}{\partial r} \bigg|_{r=1.1 \text{ in.}} = .0782$$

And from Eq. (58),

$$\Delta T(r) = 207.86 (.0782) ^\circ\text{C} \approx 16.25 ^\circ\text{C}$$

$$\Delta T(r) \approx 29.25 ^\circ\text{F} \text{ measured with laser speckle interferometry}$$

$$\Delta T(r) \approx 31 ^\circ\text{F} \text{ measured with a thermocouple}$$

Figures 24 through 27 illustrate the laboratory configuration without the cylindrical lens and front surface mirror optics present.

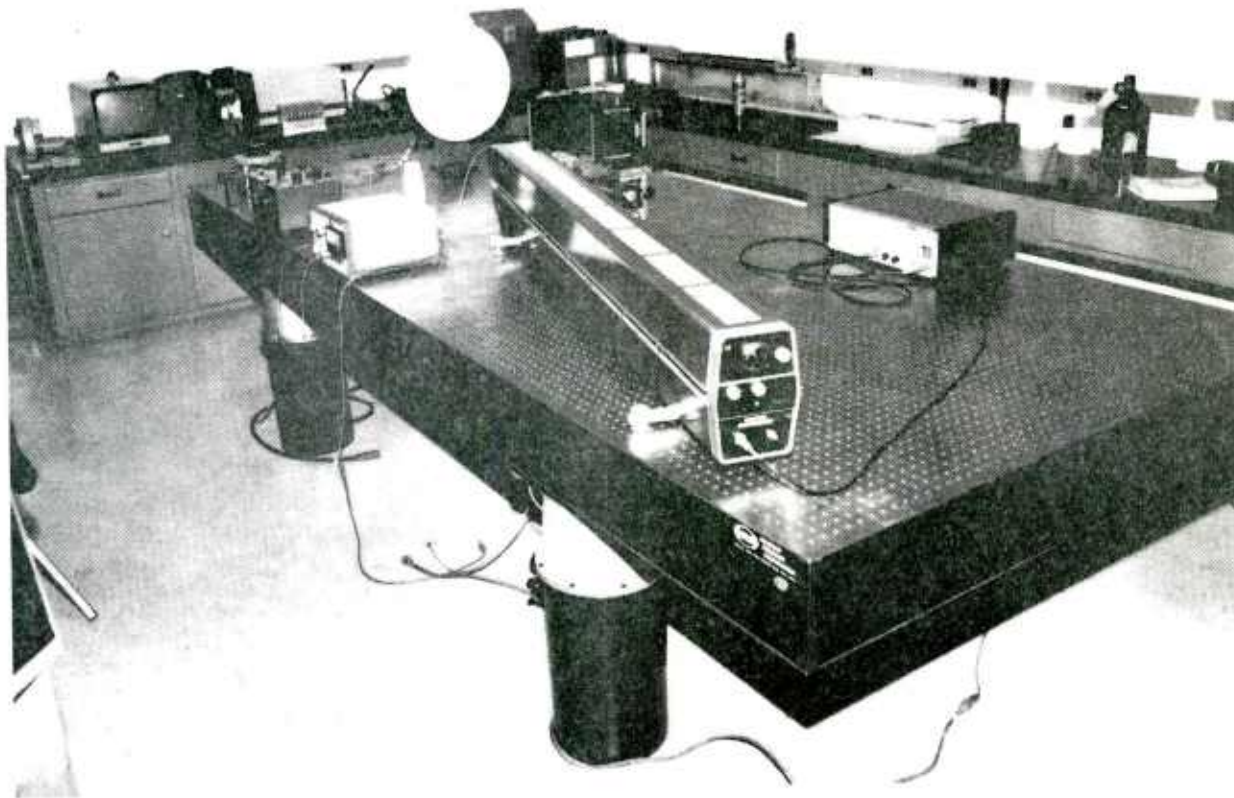


Figure 24. Illumination direction for the flat circular plate.

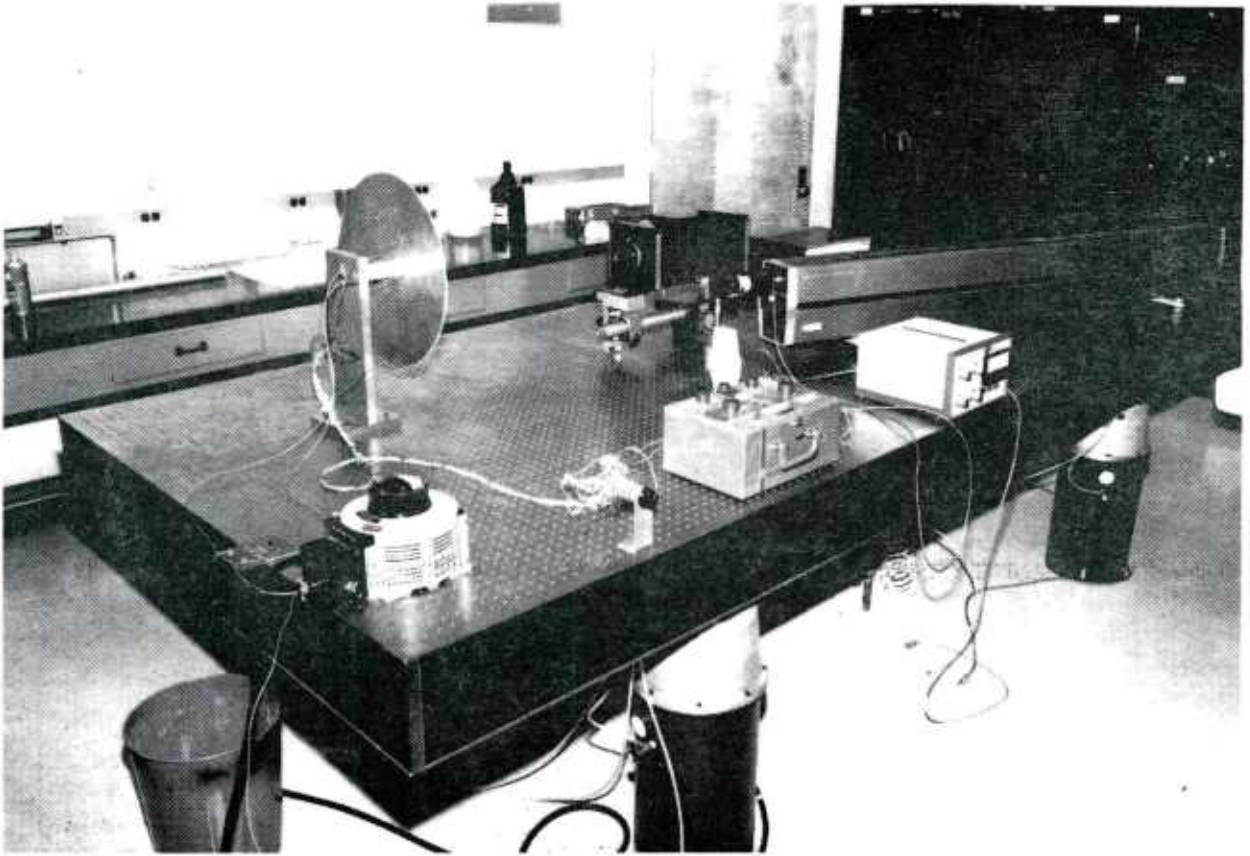


Figure 25. Side view of Case I experiment illustrating the laser, heating system, and thermocouple read-out system.

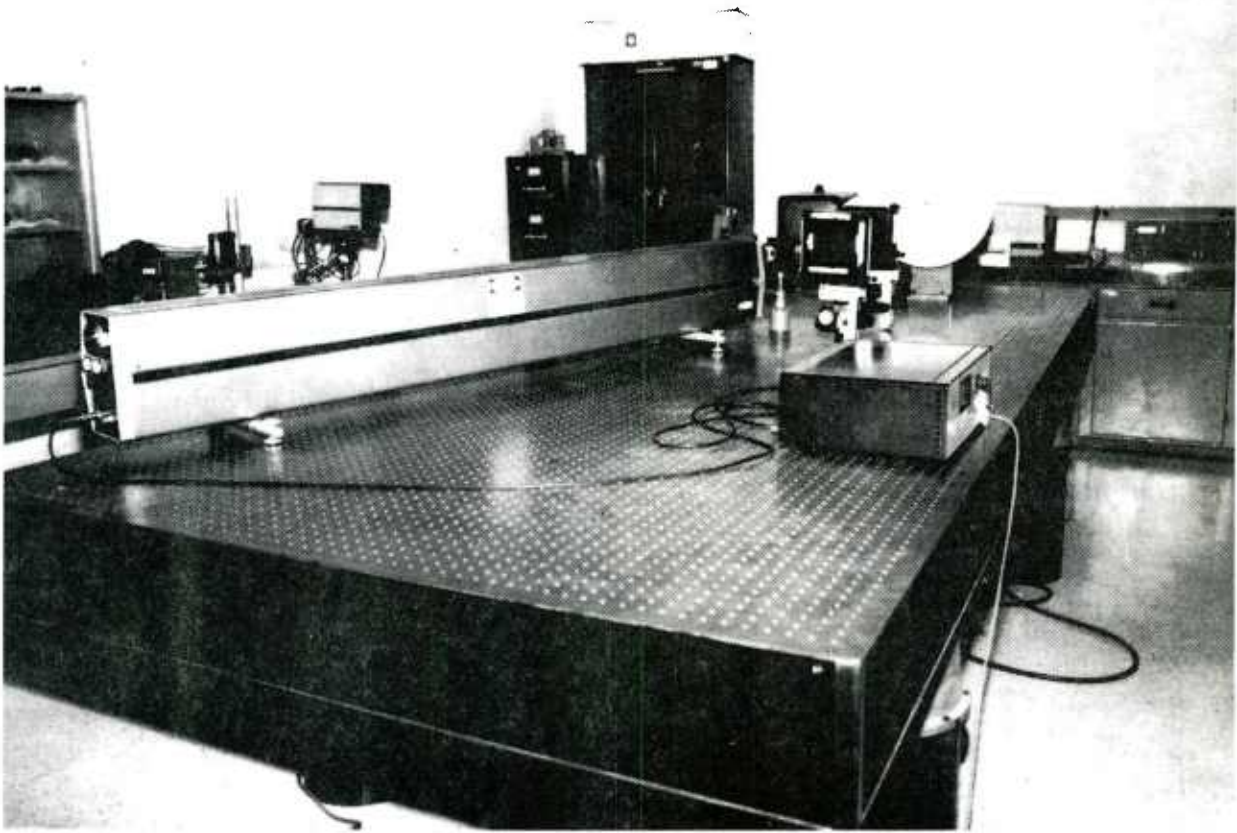


Figure 26. Case I optical configuration without cylindrical lens assembly.

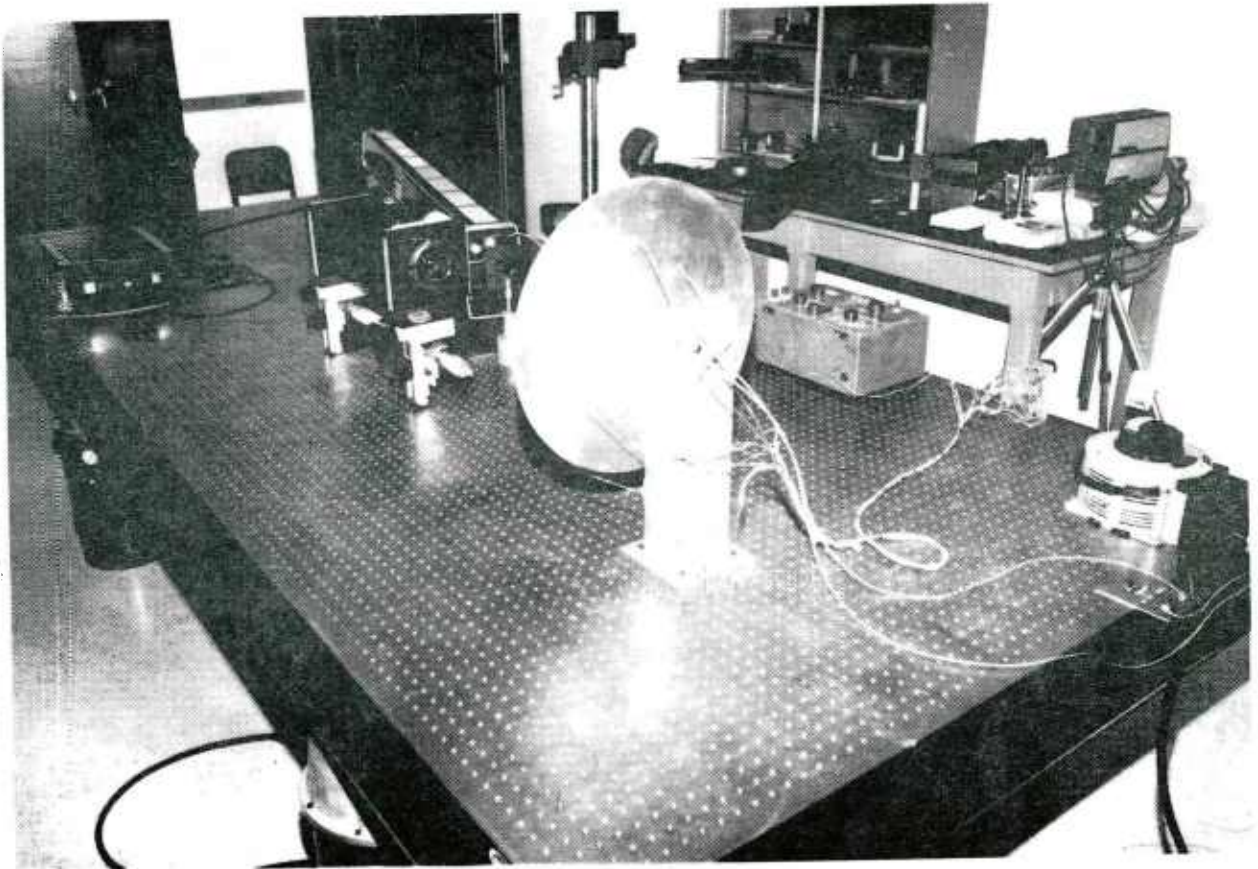


Figure 27. Back side of circular flat plate illustrating thermocouples.

C. Temperature Change Measurements for a Heated Copper Bus Bar (Case II)

In this experiment, a copper bus bar was submerged in a heated water bath and a laser speckle photograph was taken of the heated rod. The water was then replaced with cool water, and a second laser speckle photograph was taken. The double exposure interferogram was then analyzed, and the rod temperature was predicted based on various theories presented in Section II. The rod was in a state of uniform thermal contraction when cooled.

The specimen was illuminated by a Spectra-Physics 166 Argon laser operating at .9-watt power. For the test, the following data were observed:

- Initial water bath temperature = $1.280 \text{ mV} \approx 89.7^\circ \text{ F}$.
- Final water bath temperature = $.83 \text{ mV} \approx 69.9^\circ \text{ F}$.
- Bus bar dimensions $\begin{cases} \text{Length} = 9.95 \text{ in.} \\ \text{Width} = 1.00 \text{ in.} \\ \text{Depth} = 0.25 \text{ in.} \end{cases}$
- Approximately 5 in. of the bus bar was exposed in the water bath.
- AGFA 10E56 holographic emulsion film was used with two 16-sec exposures.
- $\lambda f = 2.4913 \times 10^{-5} (130) = .00323869 \text{ in.}^2$ (reconstruction of interferograms was with a He-Ne laser).

The copper bus bar is a glass beaker immersion tank, the Case II laboratory setup, and a side view of the Case II experiment are shown in Figures 28, 29, and 30, respectively.

The data obtained from the interferogram is illustrated in Table 3. For this table,

- $L \equiv$ distance from an arbitrary reference point on the interferogram
- $\rho \equiv$ longitudinal specimen deformation at location L .
- $\chi \equiv$ fringe spacing in the interferogram analyzer plane.
- $\Delta l \equiv$ net longitudinal deformation measured from the arbitrary reference.

All data was measured in the symmetry plane of the specimen.

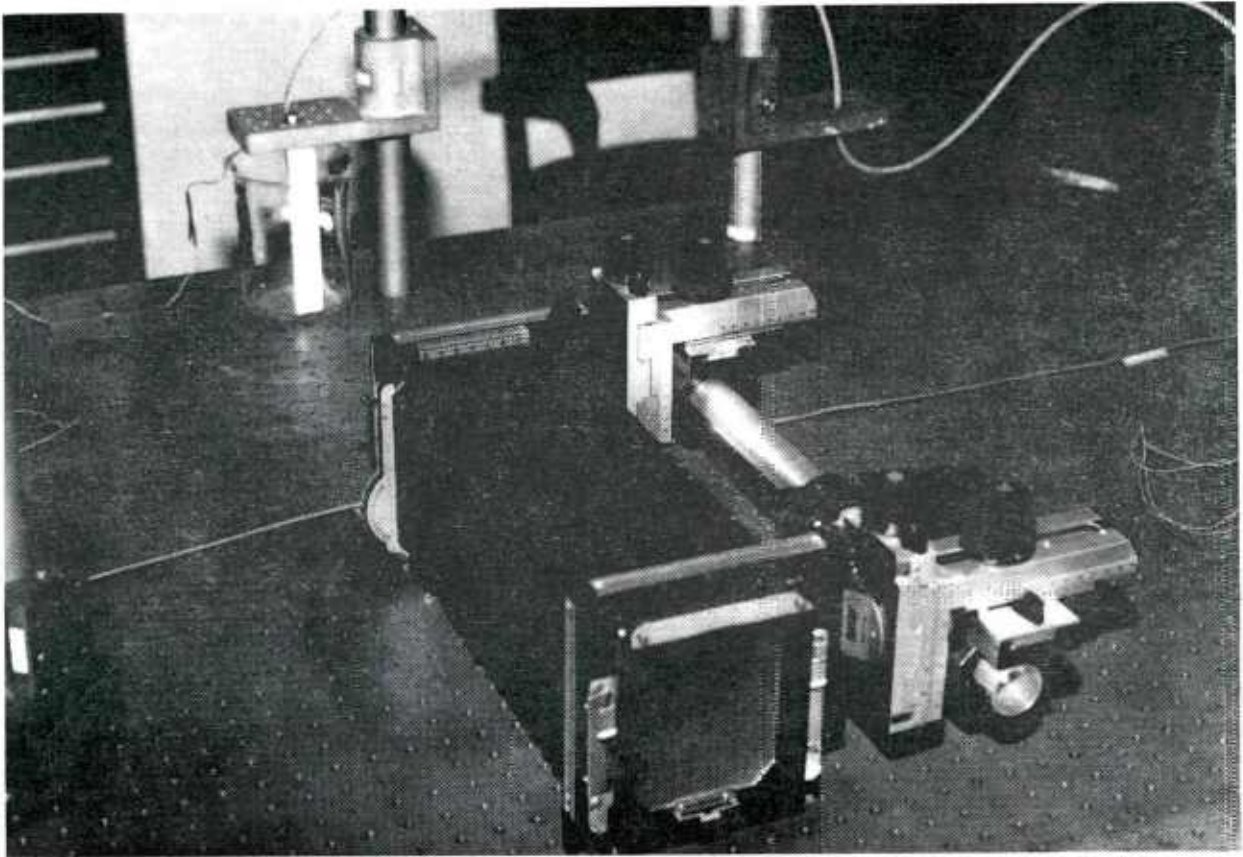


Figure 28. Copper bus bar in glass beaker immersion tank.
(Note thermocouple leads in the tank used to
monitor water temperature.)

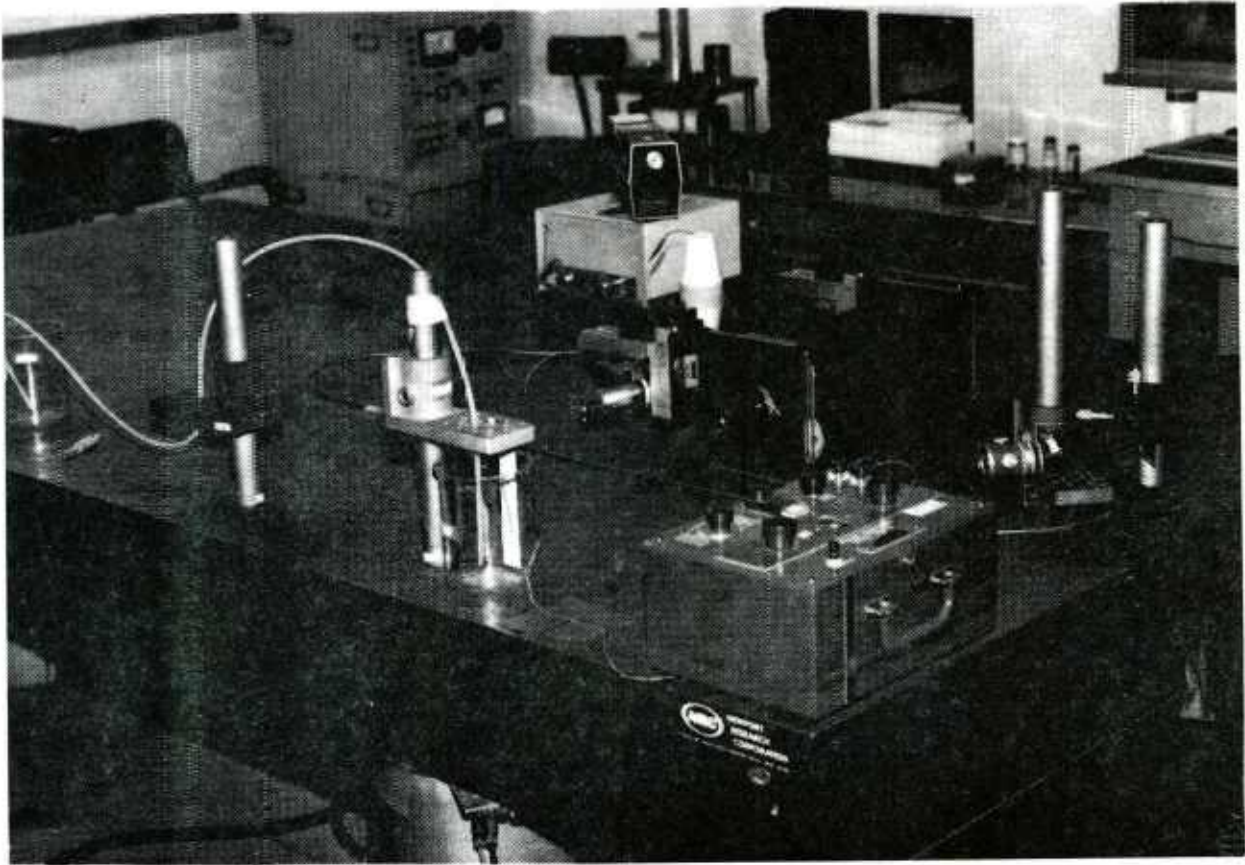


Figure 29. Case II laboratory setup.
(Note water drainage system,
thermocouple temperature read-out equipment,
and the optical system.)

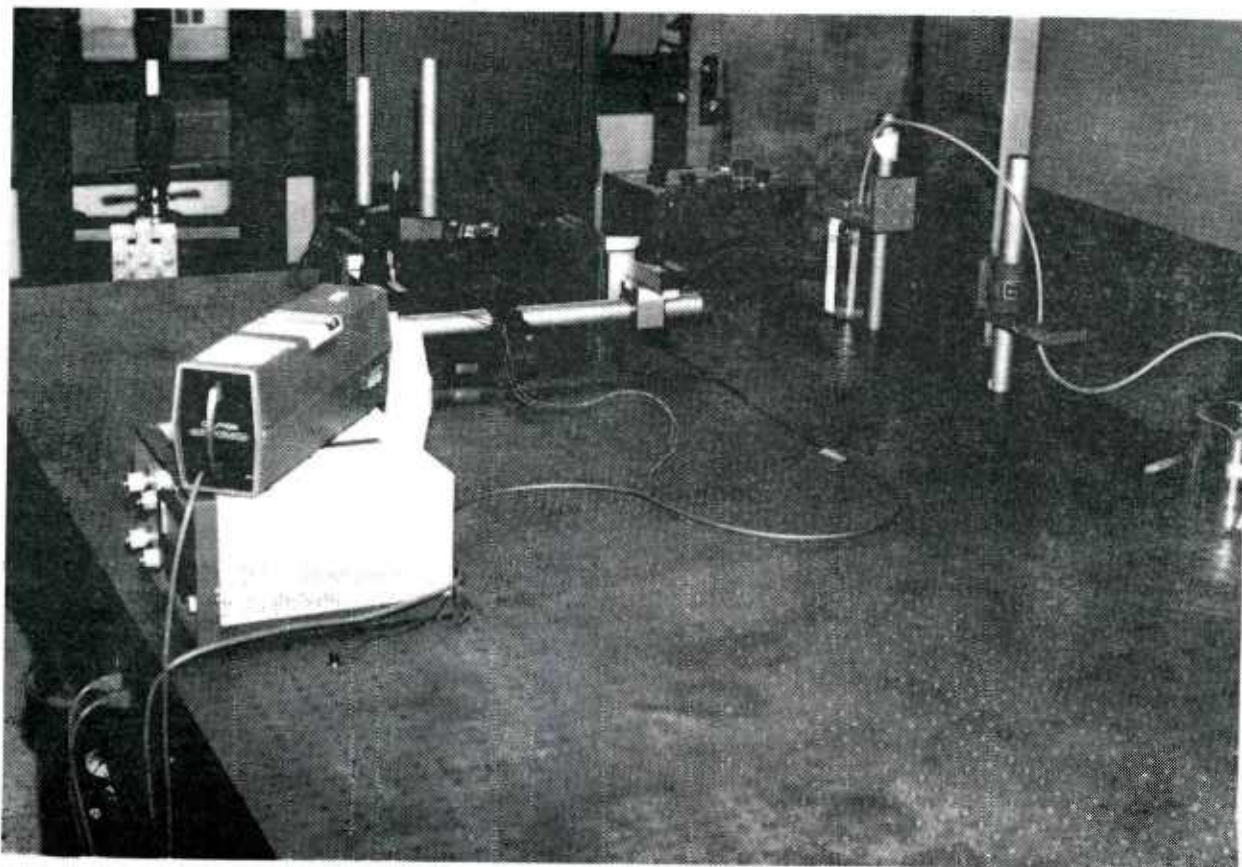


Figure 30. Side view of Case II experiment.

TABLE 3. CASE II LABORATORY DATA

L (in.)	X (in.)	ρ (in.)	$\Delta \ell = \rho - \rho_0$ (in.)
0	5.54	.0005846	0
.5	5.00	.0006477	6.310×10^{-5}
1.0	4.30	.0007531	1.685×10^{-4}
1.5	3.94	.0008220	2.374×10^{-4}
2.0	3.76	.0008613	2.767×10^{-4}

For this particular case, the temperature change can be approximated from

$$\Delta T = \frac{1}{\alpha} \frac{\Delta \ell}{L} \quad (155)$$

The results of this case are shown in Table 4, where

$$\alpha_{cu} = 7.827 \times 10^{-6}/^{\circ}\text{F}$$

$$\mu = .3$$

TABLE 4. CASE II TEMPERATURE MEASUREMENT RESULTS

L (in.)	Δl (in.)	$\frac{\Delta l}{L}$	ΔT (°F)
0	0	~	~
.5	6.310×10^{-5}	1.262×10^{-4}	16.12
1.0	1.685×10^{-4}	1.685×10^{-4}	21.52
1.5	2.374×10^{-4}	1.582×10^{-4}	20.21
2.0	2.767×10^{-4}	1.383×10^{-4}	17.66

The average temperature change computed using Eq. (155) was 18.87° F, which is about a 4.8 percent difference from the thermocouple reading of 19.8° F.

D. Temperature Change Measurements for a Heated Circular Flat Plate (Case III)

This test was identical to Case I. The data for this test case is illustrated in Table 5.

TABLE 5. CASE I TEST DATA

r (in.)	ρ_r (in.)
.30*	-.001495
1.23*	-.001228
2.44	-.001161

For the data in Table 5 marked with an asterisk, assume that

$$\rho_r = Ar + B \quad .$$

Therefore,

$$-.001495 = .3A + B$$

$$-.001228 = 1.23A + B \quad . \quad (156)$$

From Eq. (156),

$$A = 2.8709 \times 10^{-4}$$

$$B = -1.5811 \times 10^{-3} \quad .$$

B is the offset error in the data of Table 5, due to a uniform translation of the test fixture. Therefore, the ρ_r component of deformation in Table 5 should be corrected by 1.5811×10^{-3} in. to account for this uniform translation. The corrected data, ρ_r' , is illustrated in Table 6.

TABLE 6. CORRECTED TABLE 5 DATA

r	ρ_r	ρ_r'
.30	-.001495	.0000861
1.23	-.001228	.0003531
2.44	-.001161	.0004201

Now at location $r = 1.23$ in.,

$$\frac{\rho_r}{r} = \frac{3.531 \times 10^{-4}}{1.23} = 2.8707 \times 10^{-4}$$

$$\left. \frac{\partial \rho_r}{\partial r} \right|_1 = \frac{3.531 \times 10^{-4} - 8.61 \times 10^{-5}}{1.23 - .3} = 2.8709 \times 10^{-4}$$

$$\left. \frac{\partial \rho_r}{\partial r} \right|_2 = \frac{4.201 \times 10^{-4} - 3.531 \times 10^{-4}}{2.44 - 1.23} = 5.5371 \times 10^{-5}$$

$$\left. \frac{\partial \rho_r}{\partial r} \right|_{\text{avg}} = 1.7123 \times 10^{-4}$$

From Eq. (108), with $C = 0$ for an infinite plate solution,

$$\Delta T = r \left\{ \frac{\partial \rho_r}{\partial r} + \frac{\rho_r}{r} \right\} \quad (157)$$

And from the experimental data,

$$\Delta T = 65625 \left\{ 1.7123 \times 10^{-4} + 2.8707 \times 10^{-4} \right\} ^\circ \text{F}$$

$$\Delta T = 30.075^\circ \text{F at } r = 1.23 \text{ in.}$$

$$\Delta T = 31^\circ \text{F at } r = 1.10 \text{ in. (thermocouple measurement)}$$

From the above results, agreement is very good.

IV. CONCLUSIONS

The theory for laser speckle interferometric thermoelasticity was presented in Section II. Two specific problems and three methods of data analysis were presented in Section III. Laser speckle interferometry may be used to measure the in-plane deformation of a body, but no information about the out-of-plane component is obtainable. This necessarily implies that certain simplifications to the theory are needed. After making estimations for the out-of-plane component of deformation for a body, the general thermoelasticity equations are solvable.

Section III illustrates that for the case of thin plates and uniformly heated rods, accurate temperature measurements can be made. As long as the deformation of some region in a body is attributed to localized heating, then accurate temperature measurements can be made. Major problems occur when the deformation is attributed to thermostress generated elsewhere in a body. This case occurs at the outer radius of the circular flat plate where the deformation and derivatives of deformation are not zero. This is the result of thermostress generated at the center of the plate and is very difficult to analyze.

The thermostress equations usually require some form of simplification, for they involve partial derivatives of the deformation field. After a suitable set of approximations are made, the thermoelasticity equations may be made more amenable to analysis. Thermal gradient measurements are easily made, since many approximations to the deformation and temperature fields are not required.

REFERENCES

1. Westergaard, H. M., *Theory of Elasticity and Plasticity*, Dover Publications, Inc., New York, 1952.
2. Rothbart, H. A. (ed.), *Mechanical Design and Systems Handbook*, McGraw-Hill Book Co., New York, 1964.
3. Schaeffel, J. A., B. R. Mullinix, W. F. Ranson, and W. F. Swinson, *Computer Aided Optical Nondestructive Flaw Detection System for Composite Materials*, US Army Missile Research and Development Command, Redstone Arsenal, Alabama, Technical Report T-78-5, 26 September 1977.
4. Javid, M., and P. M. Brown, *Field Analysis and Electromagnetics*, McGraw-Hill Book Co., New York, 1963.
5. Wylie, J. R., *Advanced Engineering Mathematics*, McGraw-Hill Book Co., New York, 1975.

APPENDIX

Computer Codes Used to Analyze Laser Speckle Interferograms

Computer Code - 1

```

C-----CIRCULAR LASER SPECKLE INTERFEROMETRY READER
C-----WRITTEN BY: JOHN A. SCHAEFFEL, JR.
      DIMENSION XY(10,50),XX(10,50),YY(10,50)
      WRITE(5,1)
1     FORMAT(' INPUT R1,RN,T1,TM,N,M,IS-4F5.0,3I2')
      READ(5,2) R1,RN,T1,TM,N,M,IS
2     FORMAT(4F5.0,3I2)
      WRITE(5,3)
3     FORMAT(' INPUT SF,E-2F10.0')
      READ(5,4) SF,E
4     FORMAT(2F10.0)
      XL=0.
      YL=0.
      DR=(RN-R1)/FLOAT(N-1)
      DT=(TM-T1)/FLOAT(M-1)
      DO 7 I=1,M,1
      DO 7 J=1,N,1
      T=T1+FLOAT(I-1)*DT
      R=R1+FLOAT(J-1)*DR
      TP=3.14159*T/180.
      X=(R/SF)*COS(TP)
      Y=(R/SF)*SIN(TP)
      IXX=INT((X-XL)/.001)
      IYY=INT((Y-YL)/.001)
      IF(IXX.NE.0) CALL XADV(IXX,IS)
      IF(IYY.NE.0) CALL YADV(IYY,IS)
      XL=XL+FLOAT(IXX)/1000.
      YL=YL+FLOAT(IYY)/1000.
      WRITE(5,5)
5     FORMAT(' DATA-2F5.0:')
      READ(5,6) XS,FS
6     FORMAT(2F5.0)
      XY(I,J)=SF*E/XS
      XX(I,J)=XY(I,J)*COS(FS*3.14159/180.)
      YY(I,J)=XY(I,J)*SIN(FS*3.14159/180.)
7     CONTINUE
      DO 9 I=1,M,1
      DO 9 J=1,N,1
      T=T1+FLOAT(I-1)*DT
      R=(R1+FLOAT(J-1)*DR)
      WRITE(5,8) I,J,T,R,XY(I,J),XX(I,J),YY(I,J)
8     FORMAT(' I=',I3,3X,'J=',I3,3X,'ANGLE=',F8.2,3X,'R=',F8.2,3X,
1'XY=',F10.6,3X,'XX=',F10.6,3X,'YY='F10.6)
9     CONTINUE
      IXX=-INT(XL/.001)
      IYY=-INT(YL/.001)
      IF(IXX.NE.0) CALL XADV(IXX,10)
      IF(IYY.NE.0) CALL YADV(IYY,10)
      STOP
      END

```

Computer Code - 1 (Continued)

```

      SUBROUTINE YADV(IS,IR)
C-----IS=NO. STEPS (+=FWD,--=REV)
C-----IR=ADVANCE RATE OF STAGE
      X=0.
      IF(IS.GT.0) GOTO 3
      IP=IABS(IS)
      DO 2 I=1,IP,1
      CALL IPOKE("167772","020000)
      DO 7 K=1,IR,1
7      Y=SIN(X)
      CALL IPOKE("167772","000000)
      DO 1 J=1,IR,1
1      Y=SIN(X)
2      CONTINUE
      GOTO 6
3      CONTINUE
      DO 5 II=1,IS,1
      CALL IPOKE("167772","010000)
      DO 8 KK=1,IR,1
8      Y=SIN(X)
      CALL IPOKE("167772","000000)
      DO 4 JJ=1,IR,1
4      Y=SIN(X)
5      CONTINUE
6      CONTINUE
      RETURN
      END
      SUBROUTINE XADV(IS,IR)
C-----IS=NO. STEPS (+=FWD,--=REV)
C-----IR=ADVANCE RATE OF STAGE
      X=0.
      IF(IS.GT.0) GOTO 3
      IP=IABS(IS)
      DO 2 I=1,IP,1
      CALL IPOKE("167772","100000)
      DO 7 K=1,IR,1
7      Y=SIN(X)
      CALL IPOKE("167772","000000)
      DO 1 J=1,IR,1
1      Y=SIN(X)
2      CONTINUE
      GOTO 6
3      CONTINUE
      DO 5 II=1,IS,1
      CALL IPOKE("167772","040000)
      DO 8 KK=1,IR,1
8      Y=SIN(X)
      CALL IPOKE("167772","000000)
      DO 4 JJ=1,IR,1
4      Y=SIN(X)
5      CONTINUE

```

Computer Code - 2

```

C-----CYLINDRICAL COORDINATES
C-----LASER SPECKLE INTERFEROMETRY
C-----TEMPERATURE CALCULATOR CODE
C-----WRITTEN BY JOHN A. SCHAEFFEL, JR.
      DIMENSION A(2,2)
      WRITE(5,1)
1      FORMAT(' INPUT: SF,E,PSI-3F10.0')
      READ(5,2) SF,E,SI
2      FORMAT(3F10.0)
3      WRITE(5,4)
4      FORMAT(' INPUT R,THETA,DR-3F10.0')
      READ(5,2) R,T,D
      X=R*COS(T*3.14159/180.)-D
      Y=R*SIN(T*3.14159/180.)
      IX=INT(X*1000./SF)
      IY=INT(Y*1000./SF)
      IR=INT(D*1000./SF)
      IRR=2*IR
      IF(IX.NE.0) CALL XADV(IX,5)
      IF(IY.NE.0) CALL YADV(IY,5)
      DO 7 I=1,2,1
      WRITE(5,5)
5      FORMAT(' INPUT HORIZONTAL FRINGE SPACING-F5.0:')
      READ(5,6) DH
6      FORMAT(F5.0)
      A(1,I)=SF*E/DH
      CALL XADV(IRR,5)
7      CONTINUE
      IB=-3*IR
      CALL XADV(IB,5)
      IRRR=-IR
      CALL YADV(IRRR,5)
      DO 10 I=1,2,1
      WRITE(5,8)
8      FORMAT(' INPUT VERTICAL FRINGE SPACING-F5.0:')
      READ(5,9) DV
9      FORMAT(F5.0)
      A(2,I)=SF*E/DV
      CALL YADV(IRR,5)
10     CONTINUE
      CALL YADV(IB,5)
      IX=-IX-IR
      IY=-IY
      IF(IX.NE.0) CALL XADV(IX,5)
      IF(IY.NE.0) CALL YADV(IY,5)
      DT=SI*(A(1,2)-A(1,1)+A(2,2)-A(2,1))/(2.*D)
      WRITE(5,11) DT
11     FORMAT(' DELTA TEMPERATURE CHANGE=',F6.1)
      GOTO 3
      STOP
      END
      SUBROUTINE YADV(IS,IR)

```

Computer Code - 2 (Continued)

```

C-----IS=NO. STEPS (+=FWD, -=REV)
C-----IR=ADVANCE RATE OF STAGE
      X=0.
      IF (IS.GT.0) GOTO 3
      IP=IABS(IS)
      DO 2 I=1,IP,1
      CALL IPOKE("167772","020000)
      DO 7 K=1,IR,1
7      Y=SIN(X)
      CALL IPOKE("167772","000000)
      DO 1 J=1,IR,1
1      Y=SIN(X)
2      CONTINUE
      GOTO 6
3      CONTINUE
      DO 5 II=1,IS,1
      CALL IPOKE("167772","010000)
      DO 8 KK=1,IR,1
8      Y=SIN(X)
      CALL IPOKE("167772","000000)
      DO 4 JJ=1,IR,1
4      Y=SIN(X)
5      CONTINUE
6      CONTINUE
      RETURN
      END
      SUBROUTINE XADV(IS,IR)
C-----IS=NO. STEPS (+=FWD, -=REV)
C-----IR=ADVANCE RATE OF STAGE
      X=0.
      IF (IS.GT.0) GOTO 3
      IP=IABS(IS)
      DO 2 I=1,IP,1
      CALL IPOKE("167772","100000)
      DO 7 K=1,IR,1
7      Y=SIN(X)
      CALL IPOKE("167772","000000)
      DO 1 J=1,IR,1
1      Y=SIN(X)
2      CONTINUE
      GOTO 6
3      CONTINUE
      DO 5 II=1,IS,1
      CALL IPOKE("167772","040000)
      DO 8 KK=1,IR,1
8      Y=SIN(X)
      CALL IPOKE("167772","000000)
      DO 4 JJ=1,IR,1
4      Y=SIN(X)
5      CONTINUE
6      CONTINUE
      RETURN
      END

```

Computer Code - 3

```

C-----CYLINDRICAL COORDINATES
C-----LASER SPECKLE INTERFEROMETRY
C-----TEMPERATURE CALCULATOR CODE
C-----WRITTEN BY JOHN A. SCHAEFFEL, JR.
      WRITE(5,1)
1      FORMAT(' INPUT: SF,E,PSI-3F10.0')
      READ(5,2) SF,E,SI
2      FORMAT(3F10.0)
3      WRITE(5,4)
4      FORMAT(' INPUT R,THETA,DR-3F5.0')
      READ(5,5) R,T,D
5      FORMAT(3F5.0)
      X1=(R-D)*COS(T*3.14159/180.)
      Y1=(R-D)*SIN(T*3.14159/180.)
      X2=(2.*D)*COS(T*3.14159/180.)
      Y2=(2.*D)*SIN(T*3.14159/180.)
      IX1=INT(X1*1000./SF)
      IY1=INT(Y1*1000./SF)
      IX2=INT(X2*1000./SF)
      IY2=INT(Y2*1000./SF)
      IF(IX1.NE.0) CALL XADV(IX1,5)
      IF(IY1.NE.0) CALL YADV(IY1,5)
      WRITE(5,6) T
6      FORMAT(' FRINGE SPACING AT',1X,F5.1,1X,'DEGREES')
      READ(5,7) DH
7      FORMAT(F5.0)
      A=(R-D)*SF*E/DH
      IF(IX2.NE.0) CALL XADV(IX2,5)
      IF(IY2.NE.0) CALL YADV(IY2,5)
      WRITE(5,8)
8      FORMAT(' FRINGE SPACING AT',1X,F5.1,1X,'DEGREES')
      READ(5,7) DH
      B=(R+D)*SF*E/DH
      C=((B-A)/(2.*D))/R)*SI
      WRITE(5,9) C
9      FORMAT(' DELTA TEMPERATURE CHANGE=',F5.1)
      IX=-(IX1+IX2)
      IY=-(IY1+IY2)
      IF(IX.NE.0) CALL XADV(IX,5)
      IF(IY.NE.0) CALL YADV(IY,5)
      GOTO 3
      STOP
      END

```

Computer Code - 3 (Continued)

```

      SUBROUTINE YADV(IS,IR)
C-----IS=NO. STEPS (+=FWD, -=REV)
C-----IR=ADVANCE RATE OF STAGE
      X=0.
      IF(IS.GT.0) GOTO 3
      IP=IABS(IS)
      DO 2 I=1,IP,1
      CALL IPOKE("167772","020000")
      DO 7 K=1,IR,1
7      Y=SIN(X)
      CALL IPOKE("167772","000000")
      DO 1 J=1,IR,1
1      Y=SIN(X)
2      CONTINUE
      GOTO 6
3      CONTINUE
      DO 5 II=1,IS,1
      CALL IPOKE("167772","010000")
      DO 8 KK=1,IR,1
8      Y=SIN(X)
      CALL IPOKE("167772","000000")
      DO 4 JJ=1,IR,1
4      Y=SIN(X)
5      CONTINUE
6      CONTINUE
      RETURN
      END

```

```

      SUBROUTINE XADV(IS,IR)
C-----IS=NO. STEPS (+=FWD, -=REV)
C-----IR=ADVANCE RATE OF STAGE
      X=0.
      IF(IS.GT.0) GOTO 3
      IP=IABS(IS)
      DO 2 I=1,IP,1
      CALL IPOKE("167772","100000")
      DO 7 K=1,IR,1
7      Y=SIN(X)
      CALL IPOKE("167772","000000")
      DO 1 J=1,IR,1
1      Y=SIN(X)
2      CONTINUE
      GOTO 6
3      CONTINUE
      DO 5 II=1,IS,1
      CALL IPOKE("167772","040000")
      DO 8 KK=1,IR,1
8      Y=SIN(X)
      CALL IPOKE("167772","000000")
      DO 4 JJ=1,IR,1
4      Y=SIN(X)
5      CONTINUE
6      CONTINUE
      RETURN
      END

```

LIST OF SYMBOLS

A, B, C, D	Constants
B_i	Body Force Per Unit Volume
d, d_H, d_V	Fringe Spacing From Laser Speckle Interferograms
$\hat{e}_x, \hat{e}_y, \hat{e}_z$	Cartesian System Unit Vectors
$\hat{e}_r, \hat{e}_\theta, \hat{e}_z$	Cylindrical System Unit Vectors
E	Modulus of Elasticity
f	Distance Between Laser Speckle Interferogram and the Analyzer Plane
G	Lame' Constant
$\hat{i}, \hat{j}, \hat{k}$	Cartesian Unit Vectors
l, m, n	Cartesian Direction Cosines
L	Length of Specimen
m	Fringe Order
n_x, n_y, n_z	Stress Plane Direction Cosines
r, θ, z	Cylindrical Coordinates
S	Film Scale Factor
$\vec{S}_x, \vec{S}_y, \vec{S}_z$	Stress Vectors
t	Plate Thickness
u, v, w	Components of Deformation in Cartesian Coordinates
U_H, U_V	Components of Deformation Determined by Laser Speckle Interferometry
U_i	Components of Deformation in Cartesian Coordinates
x, y, z	Cartesian Coordinates
X_j	Cartesian Coordinates
α	Coefficient of Thermal Expansion

LIST OF SYMBOLS (CONCLUDED)

β	Material Constant
γ	Material Constant
Γ	Material Constant
$\Delta\epsilon$	Total Change of Length
ΔT	Temperature Change
ϵ_{ij}	Strain Tensor
ϵ_t	Thermal Strain
θ	Angle
λ	Wavelength of Light, Material Constant
μ	Poisson Ratio
$\vec{\rho}$	Deformation Vector
σ_{ij}	Stress Tensor
σ_n	Stress on Plane n
ϕ	Strain Potential
$\chi(r)$	Fringe Spacing at Radius (r)
ψ_i	Material Constants
Ω	Some Region of a Body
$\vec{\nabla}$	Gradient
$\vec{\nabla} \cdot$	Divergence
∇^2	Laplacian

DISTRIBUTION

	<u>No. of Copies</u>
Defense Technical Information Center Cameron Station Alexandria, VA 22314	12
US Army Materiel Systems Analysis Activity ATTN: DRXSY-MP Aberdeen Proving Ground, MD 21005	1
IIT Research Institute ATTN: GACIAC 10 West 35th Street Chicago, IL 60616	1
Commander US Army Foreign Science and Technology Center ATTN: DRXST-SD3 220 Seventh Street, NE Charlottesville, VA 22901	1
Defense Metals Information Center Battelle Memorial Institute 505 King Avenue Columbus, OH	1
Office of Chief of Research and Development Department of the Army ATTN: DARD-ARS-P Washington, DC 20301	1
Commander US Army Electronics Command ATTN: DRSEL-PA-P -CT-DT -PP, Mr. Sulkolove Fort Monmouth, NJ 07703	1 1 1
Commander US Army Natick Laboratories ATTN: STSNLT-EQR Kansas Street Natick, MA 01760	1

DISTRIBUTION (CONTINUED)

	<u>No. of Copies</u>
Commander US Army Mobility Equipment Research and Development Center Fort Belvoir, VA 22060	1
Director USA Mobility Equipment Research and Development Center Coating and Chemical Laboratory ATTN: STSFB-CL Aberdeen Proving Ground, MD 21005	1
Commander Edgewood Arsenal ATTN: SAREA-TS-A Aberdeen Proving Ground, MD 21010	1
Commander Picatinny Arsenal ATTN: SARPA-TS-S, Mr. M. Costello Dover, NJ 07801	1
Commander Rock Island Arsenal Research and Development ATTN: 9320 Rock Island, IL 61201	1
Commander Watervliet Arsenal Watervliet, NY 12189	1
Commander US Army Aviation Systems Command ATTN: DRSAB-EE -MT, Mr. Vollmer St. Louis, MO 63166	1 1
Commander US Army Aeronautical Depot Maintenance Center (Mail Stop) Corpus Christi, TX 78403	1

DISTRIBUTION (CONTINUED)

	<u>No. of Copies</u>
Commander US Army Test and Evaluation Command ATTN: DRSTE-RA Aberdeen Proving Ground, MD 21005	1
Commander ATTN: STEAP-MT Aberdeen Proving Ground, MD 21005	1
Chief Bureau of Naval Weapons Department of the Navy Washington, DC 20390	1
Chief Bureau of Ships Department of the Navy Washington, DC 20315	1
Naval Research Laboratory ATTN: Dr. M. M. Krafft Code 8430 Washington, DC 20375	1
Commander Wright Air Development Division ATTN: ASRC Wright-Patterson AFB, OH 45433	1
Director Air Force Materiel Laboratory ATTN: AFML-DO-Library Wright-Patterson AFB, OH 45433	1
Director Army Materials and Mechanics Research Center ATTN: DRXMR-PL -MT, Mr. Farrow Watertown, MA 02172	1 1
Commander White Sands Missile Range ATTN: STEWS-AD-L White Sands Missile Range, NM 88002	1

DISTRIBUTION (CONTINUED)

	<u>No. of Copies</u>
Deputy Commander US Army Nuclear Agency ATTN: MONA-ZB Fort Bliss, TX 79916	1
Jet Propulsion Laboratory California Institute of Technology ATTN: Library/Acquisitions 111-113 4800 Oak Grove Drive Pasadena, CA 91103	1
Sandia Laboratories ATTN: Library P.O. Box 969 Livermore, CA 94550	1
Commander US Army Air Defense School ATTN: ATSA-CD-MM Fort Bliss, TX 79916	1
Technical Library Naval Ordnance Station Indian Head, MD 20640	1
Commander US Army Materiel Development and Readiness Command ATTN: DRCMT Washington, DC 20315	1
Headquarters SAC/NRI (Stinfo Library) Offutt Air Force Base, NE 68113	1
Commander Rock Island Arsenal ATTN: SARRI-KLPL-Technical Library Rock Island, IL 61201	1
Commander (Code 233) Naval Weapons Center ATTN: Library Division China Lake, CA 93555	1

DISTRIBUTION (CONTINUED)

	<u>No. of Copies</u>
Department of the Army US Army Research Office ATTN: Information Processing Office P.O. Box 12211 Research Triangle Park, NC 27709	1
Commander US Army Research Office ATTN: DRXRO-PW, Dr. R. Lontz P.O. Box 12211 Research Triangle Park, NC 27709	2
US Army Research and Standardization Group (Europe) ATTN: DRXSN-E-RX, Dr. Alfred K. Nodoluha Box 65 FPO New York 09510	2
Headquarters Department of the Army Office of the DCS for Research Development and Acquisition ATTN: DAMA-ARZ Room 3A474, The Pentagon Washington, DC 20310	2
University of California Los Alamos Scientific Laboratory ATTN: Reports Library P.O. Box 1663 Los Alamos, NM 87545	1
ADTC (DLDSL) Eglin Air Force Base, FL 32542	1
Commander US Army Materiel Development and Readiness Command ATTN: DRCRD DRCDL 5001 Eisenhower Avenue Alexandria, VA 22333	1 1
Director Defense Advanced Research Projects Agency 1400 Wilson Boulevard Arlington, VA 22209	1

DISTRIBUTION (CONCLUDED)

	<u>No. of Copies</u>
DRSMI-LP, Mr. Voigt	1
DRSMI-E	2
-ES	1
-EM	1
-EP	1
-ET	3
DRSMI-R, Dr. Kobler	1
-RL, Mr. Comus	1
-RLA, Mr. Pettey	1
Mr. Schaeffel	50
-RPR	3
-RPT (Record Cy)	1
(Reference Cy)	1